$B^0_{d,s} \to f_1 f_1$ decays with $f_1(1285)-f_1(1420)$ mixing in the perturbative QCD approach

Zewen Jiang,[1] De-Hua Yao,[1] Zhi-Tian Zou,[2] Xin Liu,[1,*] Ying Li,[2] and Zhen-Jun Xiao[3]

[1]Department of Physics, Jiangsu Normal University, Xuzhou 221116, China
[2]Department of Physics, Yantai University, Yantai 264005, China
[3]Department of Physics and Institute of Theoretical Physics, Nanjing Normal University, Nanjing 210023, China

(Received 14 August 2020; accepted 3 November 2020; published 21 December 2020)

We investigate the $B^0_{d,s} \to f_1 f_1$ decays in the framework of perturbative QCD (PQCD) approach with a referenced value $\phi_{f_1} \sim 24°$. Here, f_1 denotes the axial-vector mesons $f_1(1285)$ and $f_1(1420)$ with mixing angle ϕ_{f_1} in the quark-flavor basis. The observables such as branching ratios, direct CP violations, and polarization fractions of the $B^0_s \to f_1 f_1$ decays are predicted for the first time. We find that (i) the almost pure penguin modes $B^0_s \to f_1 f_1$ have large branching ratios in the order of $10^{-6} \sim 10^{-5}$ due to the Cabibbo-Kobayashi-Maskawa enhancement and generally constructive interferences between the amplitudes of $B^0_s \to f_n f_s$ and $B^0_s \to f_s f_s$ with f_n and f_s being the quark-flavor states of f_1 mesons. (ii) The observables receive important contributions from the weak annihilation diagrams in the PQCD approach. In particular, without the annihilation contributions, the $B^0_s \to f_1(1420) f_1(1420)$ branching ratio will decrease about 81% and its longitudinal polarization fraction will reduce around 43%. And (iii) the dependence of the $B^0_{d,s} \to f_1 f_1$ decay rates on ϕ_{f_1} exhibits some interesting line shapes, whose confirmations would be helpful to constrain the determination of ϕ_{f_1} inversely. All the PQCD predictions await for the (near) future examinations at Large Hadron Collider beauty and/or Belle-II experiments to further understand the properties of the axial-vector mesons and the perturbative dynamics released from the considered decay modes.

DOI: 10.1103/PhysRevD.102.116015

I. INTRODUCTION

As listed in the Particle Data Group (PDG) [1], the $f_1(1285)$ and its partner, namely, the $f_1(1420)$,[1] are categorized into the light axial-vector meson family with a spin-parity quantum number $J^P = 1^+$. In the naïve quark model, according to the spectroscopic notation $n^{2S+1}L_J$ with radial excitation n, spin multiplicity $2S+1$, relative angular momentum L, and total spin J [3], they are one type of the p-wave mesons, namely, 1^3P_1. Analogous to $\eta - \eta'$ mixing in the pseudoscalar sector [1], due to SU(3) flavor symmetry breaking effects, these two f_1 mesons [for the sake of simplicity, hereafter, we will use f_1 to denote both $f_1(1285)$ and $f_1(1420)$ unless otherwise stated] also demand the admixtures of the flavor states $f_n \equiv \frac{u\bar{u}+d\bar{d}}{\sqrt{2}}$ and $f_s \equiv s\bar{s}$ in the quark-flavor basis and could be described as a 2×2 rotation matrix [4]:

$$\begin{pmatrix} f_1(1285) \\ f_1(1420) \end{pmatrix} = \begin{pmatrix} \cos\phi_{f_1} & -\sin\phi_{f_1} \\ \sin\phi_{f_1} & \cos\phi_{f_1} \end{pmatrix} \begin{pmatrix} f_n \\ f_s \end{pmatrix}, \quad (1)$$

with a mixing angle ϕ_{f_1}, which is correlated with the angle θ_{f_1} in the singlet-octet basis via the following relation,

$$\phi_{f_1} = \theta_i - \theta_{f_1}. \quad (2)$$

Here, θ_i is the "ideal" mixing angle with the value $\theta_i = 35.3°$. It is therefore clear to see that ϕ_{f_1} could be as a probe to examine the deviation from ideal mixing. On one hand, the definite understanding of this ϕ_{f_1} (or θ_{f_1}) could shed light on the structure of these two f_1 mesons. On the other hand, it is of great interest to note that, as one of the three important mixing angles in the sector of

*liuxin@jsnu.edu.cn

[1]It is noted that the $f_1(1420)$ is generally considered as the partner of the $f_1(1285)$ [1], although the authors stated that both the $f_1(1420)$ and the $f_1(1510)$ are partners of the $f_1(1285)$ [2]. In this work, we will take the $f_1(1420)$ as the partner of the $f_1(1285)$. For more information about these two axial-vector states, please refer to the mini review "63. pseudoscalar and pseudovector mesons in the 1400 MeV region" [1] in the PDG2020 for detail, and references therein.

axial-vector mesons, ϕ_{f_1} (or θ_{f_1}) has the potential to help constrain the distinct mixing between K_{1A} and K_{1B} states with angle θ_{K_1} [1,5], where the former is a $^3P_1$ state while the latter is a $^1P_1$ one. It means that the good constraints on ϕ_{f_1} (or θ_{f_1}) could indirectly pin down the θ_{K_1} to better investigate the structure of $K_1(1270)$ and $K_1(1400)$ mesons [6–10].

Up to now, there are several explorations on the ϕ_{f_1} (or θ_{f_1}) at both theoretical and experimental aspects [4–6,9,11–24]. One cannot yet determine definitely its value due to limited understanding on the nature of these two f_1 states, although, about seven years ago, the Large Hadron Collider beauty (LHCb) collaboration extracted experimentally $\phi_{f_1} = (24.0^{+3.1+0.6}_{-2.6-0.8})°$ with a twofold ambiguity from the $B^0_{d,s} \to J/\psi f_1(1285)$ decays for the first time [4]. Because there are no interferences between the flavor f_n and f_s states in this type of decay modes, this ambiguity is expected to be settled in the decay modes with significantly constructive or destructive interferences between those two flavor states, for example, in the $B_{(s)} \to f_1 P$ decays [10], the $B_{(s)} \to f_1 V$ [25] modes, and other $B_{(s)}/D_{(s)} \to f_1 M$ (M stands for the possible mesons) channels. However, it is worth pointing out that the $D_{(s)} \to f_1 M$ decays cannot yet be perturbatively calculated based on the QCD theory. Hence, those relevant $D_{(s)}$ meson decays have to be left for future studies elsewhere. In this work, we will study the $B^0_{d,s} \to f_1 f_1$ decays in the perturbative QCD (PQCD) approach [26] based on the k_T factorization theorem at leading order.[2] The significant interferences among the $B^0_{d,s} \to f_n f_n, f_n f_s$, and $f_s f_s$ decay amplitudes could be observed in the considered modes, just like those in the pseudoscalar $B^0_{d,s} \to \eta^{(\prime)}\eta^{(\prime)}$ cases [32,33]. As discussed in Ref. [10], due to the consistency between the latest calculations from Lattice QCD [24] and the current measurement from LHCb [4], we will adopt $\phi_{f_1} = 24°$ as a referenced value to make quantitative evaluations and phenomenological discussions.

In the literature, the $B^0_d \to f_1 f_1$ decays have been investigated in the QCDF approach, and the decay rates and the longitudinal polarization fractions have been collected in the Table X of Ref. [22]. However, the predicted branching ratios are too small to be measured in the near future at LHCb and/or Belle-II experiments. Compared to these Cabibbo-Kobayashi-Maskawa (CKM) suppressed $B^0_d \to f_1 f_1$ modes, the CKM favored $B^0_s \to f_1 f_1$ ones are expected to be measurable with possibly large decay rates due to the naïve enhancement of $|\frac{V_{ts}}{V_{td}}|^2 \sim 20$ for both penguin-dominated channels or of $|\frac{V_{ts}V_{tb}}{V_{ub}V_{ud}}|^2 \sim 100$ for the penguin-dominated B^0_s while the tree-dominated B^0_d decays, apart from the possibly constructive interferences in the $B^0_s \to f_1 f_1$ decays. To our best knowledge, the $B^0_s \to f_1 f_1$ decays presented in this work are studied theoretically for the first time in the literature. Moreover, as discussed in Ref. [22], power corrections in QCDF always involve troublesome end point divergences. Therefore, more parameters are introduced to parametrize the contributions arising from the nonfactorizable emission and the annihilation diagrams [34], which results in large theoretical uncertainties. Objectively speaking, the QCDF approach is a powerful tool for analyzing the B meson decays by global fitting to the data. But, the data fitting and/or model-dependent parametrization always makes it lose the predictive power more or less.

The PQCD approach we adopted in this work is one of the important and popular factorization methods based on QCD dynamics. It is known that the PQCD approach, based on the k_T factorization theorem, is free of end point divergences by keeping quarks' transverse momentum, and the Sudakov formalism makes it more self-consistent. Thus, the PQCD approach does not need to introduce any other parameters, except for the essential nonperturbative inputs, namely, wave functions or distribution amplitudes for the initial and final mesons. Note that these inputs are universal and are usually computed in the nonperturbative techniques such as QCD sum rules and lattice QCD, or extracted from the available experimental data. A distinct advantage of the PQCD approach is that one can really do the quantitative calculations of form factor, nonfactorizable emission and annihilation type diagrams, apart from the factorizable emission ones. It is worth addressing that one has realized the importance of annihilation contributions in the heavy flavor B and D meson decays, for example, the predictions of CP-violating asymmetries of $B^0_d \to \pi^\pm\pi^\mp$, $K^\pm\pi^\mp$ decays [26,35], the explanations to polarization problem of $B \to \phi K^*$ modes [36–38], and the explorations of phenomenologies of $D^0 \to \pi^\pm\pi^\mp$, $K^\pm K^\mp$ channels [39], and so forth. And what is more, the confirmation from LHCb experiment on the pure annihilation $B^0_d \to K^+K^-$ and $B^0_s \to \pi^+\pi^-$ decay rates predicted in the PQCD approach are very exciting [40,41]. Actually, the PQCD predictions for the $B \to PP$, PV, and VV decays have shown good consistency globally with the existing data within errors. It means that the PQCD approach has the unique advantage and general reliability at the aspects of calculating the hadronic matrix elements in the heavy B meson decays. The interested readers could refer to the review article [26] for more details about this PQCD approach.

II. FORMALISM AND PERTURBATIVE CALCULATIONS

The decay amplitude for $B^0_{d,s} \to f_1 f_1$ decays in the PQCD approach can be conceptually written as follows:

[2]To our knowledge, the "$\pi\pi$, $K\pi$" puzzle, e.g., [27,28], in the heavy B meson decays stimulated the development of the factorization approaches to higher order, representatively, the next-to-next-to-leading order calculations [29] in the QCD factorization (QCDF) approach [30]. The PQCD approach has also started its next-to-leading order trip gradually [28,31]. But, in fact, it is well known that, according to the perturbation theory, the contributions at leading order are usually predominant.

$$A(B^0_{d,s} \to f_1 f_1) \sim \int dx_1 dx_2 dx_3 b_1 db_1 b_2 db_2 b_3 db_3 \cdot \mathrm{Tr}[C(t)\Phi_{B^0_{d,s}}(x_1, b_1)\Phi_{f_1}(x_2, b_2)\Phi_{f_1}(x_3, b_3)H(x_i, b_i, t)S_t(x_i)e^{-S(t)}], \quad (3)$$

in which, x_i $(i = 1, 2, 3)$ is the momentum fraction of the valence quark in the initial and final state mesons; b_i is the conjugate space coordinate of the transverse momentum k_{iT}; Tr denotes the trace over Dirac and SU(3) color indices; $C(t)$ stands for the Wilson coefficients including the large logarithms $\ln(m_W/t)$ [26]; t is the largest running energy scale in hard kernel $H(x_i, b_i, t)$; and Φ is the wave function describing the hadronization of quark and antiquark to a meson (the explicit form of the involved wave functions associated with the distribution amplitudes can be found later in the Appendix). The jet function $S_t(x_i)$ comes from threshold resummation, which exhibits a strong suppression effect in the small x region [42,43], while the Sudakov factor $e^{-S(t)}$ arises from k_T resummation, which provides a strong suppression in the small k_T (or large b) region [44,45]. These resummation effects therefore guarantee the removal of the end point singularities. The detailed expressions for $S_t(x_i)$ and $e^{-S(t)}$ can be easily found in Refs. [42–45]. Note that, to keep the consistency, we will use the leading order Wilson coefficients in the following calculations. For the renormalization group evolution of the Wilson coefficients from higher scale to lower scale, we will adopt the formulas in Ref. [26] directly.

A. Perturbative calculations in the PQCD approach

For the $B^0_{d,s} \to f_1 f_1$ decays, the related weak effective Hamiltonian H_{eff} can be read as [46]

$$H_{\mathrm{eff}} = \frac{G_F}{\sqrt{2}}\left\{ V^*_{ub}V_{uq}[C_1(\mu)O^u_1(\mu) + C_2(\mu)O^u_2(\mu)] - V^*_{tb}V_{tq}\left[\sum_{i=3}^{10} C_i(\mu)O_i(\mu)\right]\right\} + \mathrm{H.c.}, \quad (4)$$

in which, $q = d$ or s, $G_F = 1.16639 \times 10^{-5}$ GeV^{-2} is the Fermi constant, V denotes the CKM matrix elements, and $C_i(\mu)$ stands for Wilson coefficients at the renormalization scale μ. The local four-quark operators $O_i(i = 1, \ldots, 10)$ are written as

(1) Tree operators

$$O^u_1 = (\bar{q}_\alpha u_\beta)_{V-A}(\bar{u}_\beta b_\alpha)_{V-A},$$
$$O^u_2 = (\bar{q}_\alpha u_\alpha)_{V-A}(\bar{u}_\beta b_\beta)_{V-A}; \quad (5)$$

(2) QCD penguin operators

$$O_3 = (\bar{q}_\alpha b_\alpha)_{V-A}\sum_{q'}(\bar{q}'_\beta q'_\beta)_{V-A},$$
$$O_4 = (\bar{q}_\alpha b_\beta)_{V-A}\sum_{q'}(\bar{q}'_\beta q'_\alpha)_{V-A},$$
$$O_5 = (\bar{q}_\alpha b_\alpha)_{V-A}\sum_{q'}(\bar{q}'_\beta q'_\beta)_{V+A},$$
$$O_6 = (\bar{q}_\alpha b_\beta)_{V-A}\sum_{q'}(\bar{q}'_\beta q'_\alpha)_{V+A}; \quad (6)$$

(3) Electroweak penguin operators

$$O_7 = \frac{3}{2}(\bar{q}_\alpha b_\alpha)_{V-A}\sum_{q'} e_{q'}(\bar{q}'_\beta q'_\beta)_{V+A},$$
$$O_8 = \frac{3}{2}(\bar{q}_\alpha b_\beta)_{V-A}\sum_{q'} e_{q'}(\bar{q}'_\beta q'_\alpha)_{V+A},$$
$$O_9 = \frac{3}{2}(\bar{q}_\alpha b_\alpha)_{V-A}\sum_{q'} e_{q'}(\bar{q}'_\beta q'_\beta)_{V-A},$$
$$O_{10} = \frac{3}{2}(\bar{q}_\alpha b_\beta)_{V-A}\sum_{q'} e_{q'}(\bar{q}'_\beta q'_\alpha)_{V-A}, \quad (7)$$

with the color indices α, β and the notations $(\bar{q}'q')_{V\pm A} = \bar{q}'\gamma_\mu(1 \pm \gamma_5)q'$. The index q' in the summation of the above operators runs through u, d, s, c, and b.

As illustrated in Fig. 1, it is easy to find that the considered $B^0_{d,s} \to f_1 f_1$ decays contain two kinds of topologies of the diagrams, namely, the emission one and the annihilation one, which include eight types of diagrams in the PQCD approach at leading order: (i) factorizable [nonfactorizable] emission diagrams Figs. 1(a) and 1(b) [Figs. 1(c) and 1(d)] in the first row; and (ii) nonfactorizable [factorizable] annihilation diagrams Figs. 1(e) and 1(f) [Figs. 1(g) and 1(h)] in the second row, respectively. With the effective Hamiltonian and various operators as shown in Eqs. (4)–(7), we can straightforwardly calculate the contributions in the PQCD approach. Hereafter, for the sake of simplicity, we will adopt F and F^{P_1} (M and M^{P_1}) to denote the factorizable (nonfactorizable) Feynman amplitudes induced by the $(V-A)(V-A)$ and $(V-A)(V+A)$ operators, and F^{P_2} (M^{P_2}) to denote the factorizable (nonfactorizable) Feynman amplitudes from the $(S-P)(S+P)$ operators, which are resulted from a Fierz transformation of the $(V-A)(V+A)$ ones.

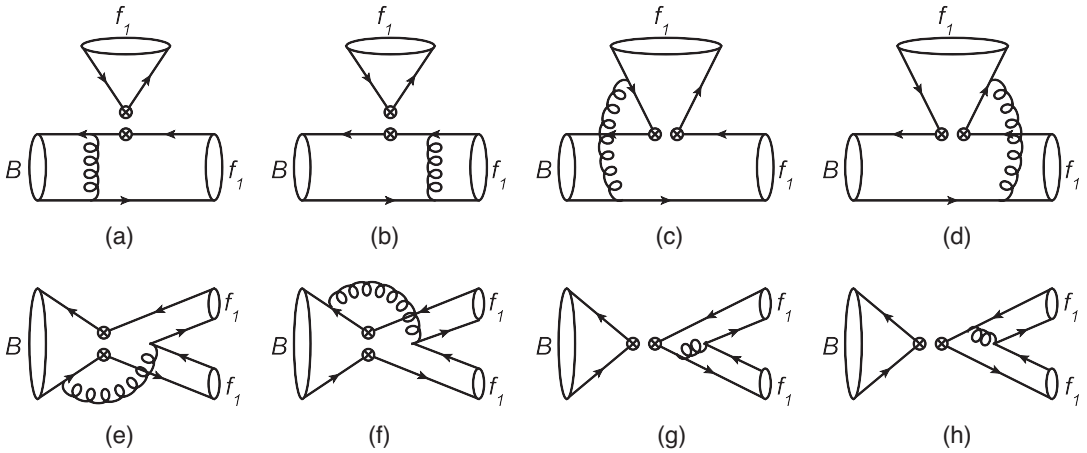

FIG. 1. Typical Feynman diagrams contributing to the $B^0_{d,s} \to f_1 f_1$ decays in the PQCD approach at leading order. Here, B and f_1 stand for the initial B^0_d and B^0_s and the final $f_1(1285)$ and $f_1(1420)$ mesons, respectively.

A remark is in order for the Feynman amplitudes: the Feynman amplitudes for the B meson decaying into two axial-vector mesons have been collected in [47]. In this work, it is not necessary for us to list the same calculations existed in the literature. The interested readers could refer to Eqs. (25)–(60) [47] for detail. In Ref. [48], the authors studied the $B_{(s)} \to VV$ decays by keeping the higher power terms proportional to $r_V^2 = m_V^2/m_B^2$ in the denominator of propagators for virtual quarks and gluons, which resulted in the predictions for most branching ratios and polarization fractions in the PQCD approach being in good agreement with the existing measurements. In light of this success, we would like to retain the terms proportional to $r_{f_1}^2 = m_{f_1}^2/m_{B^0_{d,s}}^2$ in the $B^0_{d,s} \to f_1 f_1$ decays too. In fact, we have also taken this strategy into account in the studies of $B \to f_1 V$ decays [25].

Together with various contributions from different diagrams as presented in Eqs. (25)–(60) [47] and the quark-flavor mixing scheme as shown in Eq. (1), the decay amplitudes of six $B^0_{d,s} \to f_1 f_1$ channels can thus be written in terms of the combinations of $B^0_{d,s} \to f_n f_n, f_n f_s$, and $f_s f_s$ with different coefficients as follows [the superscript h in the following formulas stands for the helicity amplitudes with longitudinal (L), normal (N), and transverse (T) polarizations, respectively]:

(1) For $B^0_d \to f_1 f_1$ decays:

The decay amplitudes for the B^0_d meson decaying into the flavor states $f_n f_n$, $f_n f_s$, and $f_s f_s$ can be easily written as follows:

$$\begin{aligned}
2A_h(B^0_d \to f_n f_n) = {} & V^*_{ub}V_{ud}\{a_2(f_{f_n}F^h_{fe} + f_{B^0_d}F^h_{fa}) + C_2(M^h_{nfe} + M^h_{nfa})\} \\
& - V^*_{tb}V_{td}\left\{\left[2a_3 + a_4 - 2a_5 - \frac{1}{2}(a_7 - a_9 + a_{10})\right] f_{f_n}F^h_{fe}\right. \\
& + \left[2a_3 + a_4 + 2a_5 + \frac{1}{2}(a_7 + a_9 - a_{10})\right] f_{B^0_d}F^h_{fa} + \left(a_6 - \frac{1}{2}a_8\right) f_{B^0_d}F^{h,P_2}_{fa} \\
& + \left[C_3 + 2C_4 - \frac{1}{2}(C_9 - C_{10})\right](M^h_{nfe} + M^h_{nfa}) \\
& \left. + \left(C_5 - \frac{1}{2}C_7\right)(M^{h,P_1}_{nfe} + M^{h,P_1}_{nfa}) + \left(2C_6 + \frac{1}{2}C_8\right)(M^{h,P_2}_{nfe} + M^{h,P_2}_{nfa})\right\},
\end{aligned} \tag{8}$$

$$\sqrt{2}A_h(B^0_d \to f_n f_s) = -V^*_{tb}V_{td}\left\{\left[a_3 - a_5 + \frac{1}{2}(a_7 - a_9)\right] f_{f_s}F^h_{fe} + \left(C_4 - \frac{1}{2}C_{10}\right)M^h_{nfe} + \left(C_6 - \frac{1}{2}C_8\right)M^{h,P_2}_{nfe}\right\}, \tag{9}$$

$$A_h(B^0_d \to f_s f_s) = -V^*_{tb}V_{td}\left\{\left[a_3 + a_5 - \frac{1}{2}(a_7 + a_9)\right] f_{B^0_d}F^h_{fa} + \left(C_4 - \frac{1}{2}C_{10}\right)M^h_{nfa} + \left(C_6 - \frac{1}{2}C_8\right)M^{h,P_2}_{nfa}\right\}. \tag{10}$$

In the above formulas, i.e., Eqs. (8)–(10), the subscripts "$(n)fe$" and "$(n)fa$" are the abbreviations of (non) factorizable emission and (non)factorizable annihilation, and a_i is the standard combination of the Wilson coefficients C_i defined as follows:

$$a_1 = C_2 + \frac{C_1}{3}, \qquad a_2 = C_1 + \frac{C_2}{3}; \tag{11}$$

$$a_i = \begin{cases} C_i + C_{i+1}/3 & (i = 3, 5, 7, 9), \\ C_i + C_{i-1}/3 & (i = 4, 6, 8, 10). \end{cases} \tag{12}$$

where $C_2 \sim 1$ is the largest one among all the Wilson coefficients.

The decay amplitudes for the physical states are then

$$A_h(B^0_d \to f_1(1285) f_1(1420)) = \sin(2\phi_{f_1})[A_h(B^0_d \to f_n f_n) - A_h(B^0_d \to f_s f_s)] + \cos(2\phi_{f_1}) A_h(B^0_d \to f_n f_s), \tag{13}$$

$$\begin{aligned} \sqrt{2} A_h(B^0_d \to f_1(1285) f_1(1285)) = {} & 2\cos^2\phi_{f_1} A_h(B^0_d \to f_n f_n) + 2\sin^2\phi_{f_1} A_h(B^0_d \to f_s f_s) \\ & - \sin(2\phi_{f_1}) A_h(B^0_d \to f_n f_s), \end{aligned} \tag{14}$$

$$\begin{aligned} \sqrt{2} A_h(B^0_d \to f_1(1420) f_1(1420)) = {} & 2\sin^2\phi_{f_1} A_h(B^0_d \to f_n f_n) + 2\cos^2\phi_{f_1} A_h(B^0_d \to f_s f_s) \\ & + \sin(2\phi_{f_1}) A_h(B^0_d \to f_n f_s). \end{aligned} \tag{15}$$

(2) For $B^0_s \to f_1 f_1$ decays:

Analogously, the decay amplitudes of $B^0_s \to f_n f_n$, $f_n f_s$, and $f_s f_s$ can be written as

$$\begin{aligned} 2A_h(B^0_s \to f_n f_n) = {} & V^*_{ub} V_{us} \{ a_2 f_{B^0_s} F^h_{fa} + C_2 M^h_{nfa} \} \\ & - V^*_{tb} V_{ts} \left\{ \left[2(a_3 + a_5) + \frac{1}{2}(a_7 + a_9) \right] f_{B^0_s} F^h_{fa} \right. \\ & \left. + \left(2C_4 + \frac{1}{2} C_{10} \right) M^h_{nfa} + \left(2C_6 + \frac{1}{2} C_8 \right) M^{h,P_2}_{nfa} \right\}, \end{aligned} \tag{16}$$

$$\begin{aligned} \sqrt{2} A_h(B^0_s \to f_n f_s) = {} & V^*_{ub} V_{us} \{ a_2 f_{f_n} F^h_{fe} + C_2 M^h_{nfe} \} \\ & - V^*_{tb} V_{ts} \left\{ \left[2(a_3 - a_5) - \frac{1}{2}(a_7 - a_9) \right] f_{f_n} F^h_{fe} \right. \\ & \left. + \left(2C_4 + \frac{1}{2} C_{10} \right) M^h_{nfe} + \left(2C_6 + \frac{1}{2} C_8 \right) M^{h,P_2}_{nfe} \right\}, \end{aligned} \tag{17}$$

$$\begin{aligned} A_h(B^0_s \to f_s f_s) = {} & -V^*_{tb} V_{ts} \left\{ \left[a_3 + a_4 - a_5 + \frac{1}{2}(a_7 - a_9 - a_{10}) \right] f_{f_s} F^h_{fe} \right. \\ & + \left[a_3 + a_4 + a_5 - \frac{1}{2}(a_7 + a_9 + a_{10}) \right] f_{B^0_s} F^h_{fa} \\ & + \left(a_6 - \frac{1}{2} a_8 \right) f_{B^0_s} F^{h,P_2}_{fa} + \left[C_3 + C_4 - \frac{1}{2}(C_9 + C_{10}) \right] \\ & \times (M^h_{nfe} + M^h_{nfa}) + \left(C_5 - \frac{1}{2} C_7 \right) (M^{h,P_1}_{nfe} + M^{h,P_1}_{nfa}) \\ & \left. + \left(C_6 - \frac{1}{2} C_8 \right) (M^{h,P_2}_{nfe} + M^{h,P_2}_{nfa}) \right\}. \end{aligned} \tag{18}$$

Then we could give the decay amplitudes for the physical states similarly,

$$A_h(B_s^0 \to f_1(1285)f_1(1420)) = \sin(2\phi_{f_1})[A_h(B_s^0 \to f_n f_n) - A_h(B_s^0 \to f_s f_s)] + \cos(2\phi_{f_1})A_h(B_s^0 \to f_n f_s), \quad (19)$$

$$\sqrt{2}A_h(B_s^0 \to f_1(1285)f_1(1285)) = 2\cos^2\phi_{f_1}A_h(B_s^0 \to f_n f_n) - \sin(2\phi_{f_1})A_h(B_s^0 \to f_n f_s) + 2\sin^2\phi_{f_1}A_h(B_s^0 \to f_s f_s), \quad (20)$$

$$\sqrt{2}A_h(B_s^0 \to f_1(1420)f_1(1420)) = 2\sin^2\phi_{f_1}A_h(B_s^0 \to f_n f_n) + \sin(2\phi_{f_1})A_h(B_s^0 \to f_n f_s) + 2\cos^2\phi_{f_1}A_h(B_s^0 \to f_s f_s). \quad (21)$$

III. NUMERICAL RESULTS AND DISCUSSIONS

Now, we will perform the numerical calculations in the PQCD approach on the experimental observables such as the CP-averaged branching ratios ($\mathcal{B}$), the direct CP-violating asymmetries ($\mathcal{A}_{CP}^{\rm dir}$), and the CP-averaged polarization fractions, etc. for the considered $B_{d,s}^0 \to f_1 f_1$ decays. Some essential comments on the input parameters are in order:

(a) Distribution amplitudes for the flavor states f_n and f_s

As discussed in [23], the $^3P_1$-axial-vector meson has the similar behavior to the vector one. Meanwhile, it is noted that, for the distribution amplitudes, the flavor η_n and η_s states of $\eta^{(\prime)}$ usually took the same form as pion but with different decay constants f_{η_n} and f_{η_s} in the pseudoscalar sector. Therefore, for the flavor states f_n and f_s in this work, we shall adopt the same distribution amplitudes as those of the $a_1(1260)$ meson. The decay constants f_{f_n} and f_{f_s}, and the relevant Gegenbauer moments can be easily found in Refs. [9,23,25,49,50].

(b) Wolfenstein parametrization of CKM matrix and four parameters

For the CKM matrix elements, we adopt the Wolfenstein parametrization at leading order [51] and the updated parameters released in PDG2018: $A = 0.836$, $\lambda = 0.22453$, $\bar{\rho} = 0.122^{+0.018}_{-0.017}$, and $\bar{\eta} = 0.355^{+0.012}_{-0.011}$ [52].

(c) QCD scale, masses, and $B_{d,s}^0$ meson lifetimes

The relevant QCD scale (GeV), masses (GeV), and B meson lifetime (ps) are the following [4,23,26,50,52]:

$$\begin{aligned}
&\Lambda_{\overline{\rm MS}}^{(f=4)} = 0.250, \quad m_W = 80.41, \quad m_{B_d^0} = 5.28,\\
&m_{B_s^0} = 5.37, \quad m_b = 4.8;\\
&f_{f_n} = 0.193^{+0.043}_{-0.038}, \quad f_{f_s} = 0.230 \pm 0.009,\\
&m_{f_n} = 1.28, \quad m_{f_s} = 1.42;\\
&\tau_{B_d^0} = 1.520, \quad \tau_{B_s^0} = 1.509,\\
&\phi_{f_1} = (24.0^{+3.2}_{-2.7})^\circ. \quad (22)
\end{aligned}$$

Of course, in numerical calculations, central values of the above input parameters will be used implicitly unless otherwise stated.

A. CP-averaged branching ratios

Similar to the $B \to f_1 V$ decays [25], the $B_{d,s}^0 \to f_1 f_1$ decay rate can also be written as

$$\Gamma = \frac{G_F^2|\mathbf{P_c}|}{16\pi m_{B_{d,s}^0}^2}\sum_{h=L,N,T} A_h^\dagger A_h, \quad (23)$$

where $|\mathbf{P_c}| \equiv |\mathbf{P_{2z}}| = |\mathbf{P_{3z}}|$ is the momentum of either the outgoing axial-vector meson and A_h can be found, for example, in Eqs. (19)–(21). The corresponding branching ratios $\mathcal{B}$ can thus be easily obtained through the relation $\mathcal{B} = \tau_{B_{d,s}^0}\Gamma$.

The numerical results predicted in the PQCD approach for the observables, specifically, branching ratios, direct CP violations, and polarization fractions associated with the theoretical errors are collected in Tables I–III. As for the errors, they are mainly induced by the uncertainties of the shape parameter $\omega_B = 0.40 \pm 0.04 (\omega_B = 0.50 \pm 0.05)$ GeV in the $B_d^0(B_s^0)$ meson distribution amplitude, of the combined decay constants f_M from the $^3P_1$-axial-vector state as $f_{f_n} = 0.193^{+0.043}_{-0.038}$ GeV and $f_{f_s} = 0.230 \pm 0.009$ GeV, of the combined Gegenbauer moments a_{f_1} from $a_2^\parallel$ and $a_1^\perp$ in the f_n and f_s state distribution amplitudes, of the mixing angle $\phi_{f_1} = (24.0^{+3.2}_{-2.7})^\circ$ for the $f_1(1285) - f_1(1420)$ mixing system in the quark-flavor basis, of the maximal running hard scale $t_{\rm max} = (1.0 \pm 0.2)t$,[3] and of the combined CKM matrix elements V from the parameters $\bar{\rho}$ and $\bar{\eta}$, respectively. Note that the errors induced by the hadronic parameters such as the decay constants and the Gegenbauer

[3]As mentioned above, parts of the next-to-leading order corrections to two-body hadronic B meson decays have been proposed in the PQCD approach [28,31], however, the higher order QCD contributions to the decays of B mesons into two vector final states beyond leading order are not yet available now. Therefore, the higher order contributions in this work are simply investigated by exploring the variation of hard scale $t_{\rm max}$ with 20%, i.e., from $0.8t$ to $1.2t$ (not changing $1/b_i$, $i = 1, 2, 3$), in the hard kernel, which have been counted into one of the sources of theoretical uncertainties. As can be seen in the Tables I–III, it looks like that, relative to the color-suppressed, tree-dominated $B_d^0 \to f_1(1285)f_1(1285)$ mode, all the other five decays considered in this work are more sensitive to the higher order corrections potentially.

moments in the adopted distribution amplitudes, particularly for the axial-vector states, are larger than those from other inputs, which can be easily seen from the Tables I–III. Frankly speaking, due to the lack of the essential constraints from experiments, we have to choose the available parameters calculated in the QCD sum rules with large uncertainties. Therefore, it is expected that the experimental examinations on the numerical results and the theoretical predictions presented in this work could provide effective constraints on these hadronic parameters in the (near) future. Meanwhile, the calculations of the above-mentioned inputs arising from lattice QCD could also help better understand the relevant hadron dynamics and give more precise predictions theoretically.

Based on the effective Hamiltonian as shown in Eq. (4), it is clear to see that, at the quark level, the $B^0_d \to f_1 f_1$ decays are the $\Delta S = 0$ (here, the capital S describes the strange flavor number) type modes with the $\bar{b} \to \bar{d}$ transition, while the $B^0_s \to f_1 f_1$ ones are the $\Delta S = 1$ type channels with the $\bar{b} \to \bar{s}$ transition, where the former is CKM suppressed, and the latter is, however, CKM favored. Then, as generally expected, the $B^0_s \to f_1 f_1$ decay rates are much larger than the $B^0_d \to f_1 f_1$ ones with different extents due to the CKM enhancement and the constructive/destructive interferences among the flavor $f_n f_n$, $f_n f_s$, and $f_s f_s$ final states. The $\mathcal{B}(B^0_{d,s} \to f_1 f_1)$ predicted in the PQCD approach can confirm this expectation numerically. One can see the predictions as presented explicitly in the Tables I–III. Within a bit large theoretical uncertainties, the branching ratios of $B^0_{d,s} \to f_1 f_1$ decays in the PQCD approach can be read as follows,

TABLE I. Theoretical predictions on the quantities of the $B^0_{d,s} \to f_1(1285) f_1(1420)$ decays obtained in the PQCD approach, where the errors are sequentially from the shape parameter ω_B, the decay constants f_M, the Gegenbauer moments a_{f_1}, the mixing angle ϕ_{f_1}, the higher order corrections factor a_t, and the CKM parameters V.

Decay modes		$B^0_d \to f_1(1285) f_1(1420)$	$B^0_s \to f_1(1285) f_1(1420)$
$\mathcal{B}$	$\Gamma/\Gamma_{\text{total}}$	$5.05^{+1.14+4.73+3.00+0.23+1.21+0.11}_{-0.87-2.47-1.92-0.26-0.73-0.09} \times 10^{-7}$	$7.50^{+1.56+1.26+6.25+1.08+1.97+0.01}_{-1.03-1.10-4.16-0.70-1.31-0.01} \times 10^{-6}$
$f_L(\%)$	$\lvert\mathcal{A}_L\rvert^2$	$18.0^{+0.8+4.8+13.0+0.8+2.2+0.8}_{-0.4-2.5-5.4-0.6-0.4-0.6}$	$59.0^{+6.4+3.4+2.6+6.0+2.2+0.0}_{-6.6-5.3-4.9-8.4-3.2-0.0}$
$f_{\lvert\rvert}(\%)$	$\lvert\mathcal{A}_{\lvert\rvert}\rvert^2$	$45.3^{+0.3+1.5+3.5+0.3+0.5+0.4}_{-0.4-2.4-7.8-0.2-1.3-0.3}$	$23.2^{+3.8+3.0+2.8+4.8+1.9+0.1}_{-3.6-1.9-1.5-3.4-1.2-0.0}$
$f_\perp(\%)$	$\lvert\mathcal{A}_\perp\rvert^2$	$36.6^{+0.2+1.2+2.0+0.5+0.0+0.4}_{-0.3-2.2-5.0-0.4-0.7-0.4}$	$17.7^{+2.9+2.3+2.2+3.6+1.4+0.0}_{-2.7-1.4-1.2-2.5-0.9-0.0}$
$\phi_{\lvert\rvert}$(rad)	$\arg\frac{\mathcal{A}_{\lvert\rvert}}{\mathcal{A}_L}$	$1.89^{+1.40+2.00+2.62+0.27+0.14+2.15}_{-0.00-0.00-0.00-0.00-0.00-0.00}$	$1.99^{+0.16+0.22+0.11+0.22+0.08+0.01}_{-0.17-0.29-0.21-0.24-0.05-0.00}$
$\phi_\perp$(rad)	$\arg\frac{\mathcal{A}_\perp}{\mathcal{A}_L}$	$1.92^{+1.40+2.00+1.54+1.37+0.98+0.07}_{-0.00-0.00-0.10-0.00-0.00-0.07}$	$2.00^{+0.16+0.25+0.11+0.23+0.08+0.00}_{-0.16-0.29-0.20-0.24-0.05-0.00}$
$\mathcal{A}^{\text{dir}}_{CP}(\%)$	$\frac{\bar{\Gamma}-\Gamma}{\bar{\Gamma}+\Gamma}$	$54.7^{+0.9+1.5+2.8+2.5+0.5+1.4}_{-1.4-3.1-8.6-2.7-2.8-1.3}$	$2.8^{+0.2+0.0+0.8+0.0+0.0+0.1}_{-0.3-0.3-0.7-0.3-0.0-0.1}$
$\mathcal{A}^{\text{dir}}_{CP}(L)(\%)$	$\frac{\bar{f}_L-f_L}{f_L+f_L}$	$94.8^{+0.0+0.7+2.6+0.0+1.1+1.2}_{-1.4-10.2-23.9-2.0-11.9-1.4}$	$-5.0^{+0.3+1.1+1.4+0.5+0.0+0.1}_{-0.3-1.5-2.8-0.5-0.2-0.2}$
$\mathcal{A}^{\text{dir}}_{CP}(\lvert\rvert)(\%)$	$\frac{\bar{f}_{\lvert\rvert}-f_{\lvert\rvert}}{f_{\lvert\rvert}+f_{\lvert\rvert}}$	$46.3^{+0.7+3.4+5.7+3.6+2.4+1.5}_{-1.1-4.2-5.7-3.5-3.5-1.6}$	$13.6^{+1.9+3.3+0.2+3.1+1.0+0.5}_{-1.9-3.6-1.1-3.7-1.2-0.4}$
$\mathcal{A}^{\text{dir}}_{CP}(\perp)(\%)$	$\frac{\bar{f}_\perp-f_\perp}{f_\perp+f_\perp}$	$45.5^{+0.8+3.0+3.0+3.3+2.2+1.5}_{-1.2-3.7-4.6-3.2-3.4-1.6}$	$14.8^{+1.9+3.6+0.9+3.3+1.2+0.5}_{-2.0-4.0-1.5-4.1-1.4-0.5}$

TABLE II. Same as Table I but for $B^0_{d,s} \to f_1(1285) f_1(1285)$ decays.

Decay modes		$B^0_d \to f_1(1285) f_1(1285)$	$B^0_s \to f_1(1285) f_1(1285)$
$\mathcal{B}$	$\Gamma/\Gamma_{\text{total}}$	$6.64^{+1.21+8.12+2.68+0.51+0.80+0.35}_{-0.96-3.82-1.40-0.60-0.38-0.31} \times 10^{-7}$	$3.70^{+1.30+2.15+2.11+0.70+0.95+0.02}_{-0.90-1.34-1.55-0.54-0.66-0.01} \times 10^{-6}$
$f_L(\%)$	$\lvert\mathcal{A}_L\rvert^2$	$27.7^{+3.4+3.7+18.2+2.3+5.0+0.4}_{-3.4-2.5-9.9-1.7-3.4-0.4}$	$78.9^{+1.7+1.5+4.6+1.1+0.0+0.1}_{-1.8-1.7-7.0-1.2-0.1-0.2}$
$f_{\lvert\rvert}(\%)$	$\lvert\mathcal{A}_{\lvert\rvert}\rvert^2$	$38.2^{+1.9+1.8+6.0+0.9+2.2+0.2}_{-1.9-2.0-10.3-1.3-2.9-0.2}$	$11.7^{+1.0+0.9+3.8+0.6+0.1+0.1}_{-1.0-0.8-2.6-0.6-0.0-0.1}$
$f_\perp(\%)$	$\lvert\mathcal{A}_\perp\rvert^2$	$34.1^{+1.5+1.1+4.0+0.7+1.2+0.2}_{-1.5-1.7-8.0-1.1-2.1-0.2}$	$9.4^{+0.8+0.8+3.3+0.5+0.1+0.1}_{-0.7-0.7-2.1-0.5-0.0-0.0}$
$\phi_{\lvert\rvert}$ (rad)	$\arg\frac{\mathcal{A}_{\lvert\rvert}}{\mathcal{A}_L}$	$4.10^{+0.02+0.04+0.11+0.03+0.17+0.03}_{-0.03-0.06-1.38-0.04-0.09-0.02}$	$4.00^{+0.15+0.25+0.16+0.15+0.05+0.00}_{-0.13-0.16-0.13-0.11-0.02-0.00}$
$\phi_\perp$ (rad)	$\arg\frac{\mathcal{A}_\perp}{\mathcal{A}_L}$	$4.11^{+0.02+0.05+0.11+0.04+0.18+0.03}_{-0.02-0.07-1.41-0.04-0.09-0.02}$	$4.02^{+0.15+0.24+0.16+0.15+0.04+0.00}_{-0.13-0.16-0.13-0.11-0.03-0.00}$
$\mathcal{A}^{\text{dir}}_{CP}(\%)$	$\frac{\bar{\Gamma}-\Gamma}{\bar{\Gamma}+\Gamma}$	$26.5^{+0.7+5.1+10.8+3.5+1.7+0.9}_{-0.8-7.3-17.7-4.5-2.5-0.9}$	$-0.3^{+0.5+0.7+0.8+0.5+0.2+0.0}_{-0.4-0.5-1.1-0.3-0.1-0.0}$
$\mathcal{A}^{\text{dir}}_{CP}(L)(\%)$	$\frac{\bar{f}_L-f_L}{f_L+f_L}$	$-72.0^{+7.8+5.2+28.1+3.3+17.1+2.4}_{-8.3-4.0-19.5-2.8-17.6-2.2}$	$-2.8^{+0.2+0.3+0.9+0.2+0.4+0.1}_{-0.0-0.2-0.9-0.1-0.3-0.0}$
$\mathcal{A}^{\text{dir}}_{CP}(\lvert\rvert)(\%)$	$\frac{\bar{f}_{\lvert\rvert}-f_{\lvert\rvert}}{f_{\lvert\rvert}+f_{\lvert\rvert}}$	$66.3^{+4.3+0.4+0.0+0.4+1.5+2.3}_{-4.7-1.4-9.9-0.8-1.7-2.5}$	$9.1^{+3.1+5.3+2.6+3.4+0.5+0.3}_{-2.6-4.0-3.7-2.7-0.3-0.3}$
$\mathcal{A}^{\text{dir}}_{CP}(\perp)(\%)$	$\frac{\bar{f}_\perp-f_\perp}{f_\perp+f_\perp}$	$62.0^{+4.1+0.6+1.1+0.4+2.0+2.3}_{-4.3-1.3-10.3-0.7-2.0-2.1}$	$8.6^{+3.1+5.7+2.6+3.6+0.7+0.3}_{-2.6-4.2-3.6-2.8-0.4-0.3}$

TABLE III. Same as Table I but for $B^0_{d,s} \to f_1(1420)f_1(1420)$ decays.

Decay modes		$B^0_d \to f_1(1420)f_1(1420)$	$B^0_s \to f_1(1420)f_1(1420)$
$\mathcal{B}$	$\Gamma/\Gamma_{\rm total}$	$1.00^{+0.20+0.75+0.59+0.33+0.23+0.00}_{-0.14-0.42-0.33-0.23-0.15-0.00} \times 10^{-7}$	$3.37^{+0.29+0.58+3.04+0.12+1.01+0.01}_{-0.24-0.50-2.00-0.17-0.65-0.00} \times 10^{-5}$
$f_L(\%)$	$\lvert\mathcal{A}_L\rvert^2$	$12.4^{+5.1+5.4+19.5+2.7+3.4+0.2}_{-3.9-1.9-6.0-1.5-2.8-0.2}$	$10.6^{+1.6+1.5+9.8+0.9+1.9+0.0}_{-1.8-1.4-3.3-1.0-1.8-0.0}$
$f_{\lvert\rvert}(\%)$	$\lvert\mathcal{A}_{\lvert\rvert}\rvert^2$	$49.7^{+2.3+0.9+3.9+0.8+1.8+0.2}_{-3.0-3.1-11.7-1.5-2.1-0.2}$	$51.1^{+1.0+0.7+2.2+0.5+1.0+0.0}_{-0.9-0.9-6.4-0.6-1.1-0.0}$
$f_\perp(\%)$	$\lvert\mathcal{A}_\perp\rvert^2$	$37.9^{+1.7+0.9+2.2+0.7+1.1+0.1}_{-2.1-2.4-7.7-1.2-1.3-0.0}$	$38.3^{+0.9+0.7+1.1+0.5+0.7+0.0}_{-0.7-0.6-3.4-0.3-0.7-0.0}$
$\phi_{\lvert\rvert}$ (rad)	$\arg\frac{\mathcal{A}_{\lvert\rvert}}{\mathcal{A}_L}$	$4.22^{+0.20+0.10+0.34+0.08+0.22+0.00}_{-0.14-0.18-1.25-0.11-0.16-0.01}$	$3.37^{+0.00+0.09+0.05+0.06+0.13+0.00}_{-0.01-0.09-0.06-0.06-0.10-0.00}$
$\phi_\perp$ (rad)	$\arg\frac{\mathcal{A}_\perp}{\mathcal{A}_L}$	$4.25^{+0.20+0.10+0.34+0.08+0.22+0.00}_{-0.11-0.18-1.25-0.11-0.16-0.01}$	$3.40^{+0.00+0.09+0.05+0.06+0.13+0.00}_{-0.01-0.09-0.06-0.06-0.10-0.00}$
$\mathcal{A}^{\rm dir}_{CP}(\%)$	$\frac{\bar\Gamma-\Gamma}{\bar\Gamma+\Gamma}$	$25.4^{+1.8+6.9+5.0+5.0+3.2+0.8}_{-2.2-8.3-11.9-4.9-3.0-0.7}$	$-1.9^{+0.2+0.3+0.4+0.2+0.2+0.1}_{-0.2-0.3-0.6-0.2-0.2-0.1}$
$\mathcal{A}^{\rm dir}_{CP}(L)(\%)$	$\frac{\bar f_L-f_L}{\bar f_L+f_L}$	$9.4^{+19.1+25.9+39.7+18.3+11.9+0.4}_{-9.4-20.6-67.8-14.0-17.7-0.4}$	$2.3^{+0.6+0.1+0.8+0.1+0.7+0.0}_{-0.5-0.4-0.6-0.2-0.7-0.1}$
$\mathcal{A}^{\rm dir}_{CP}(\lvert\rvert)(\%)$	$\frac{\bar f_{\lvert\rvert}-f_{\lvert\rvert}}{\bar f_{\lvert\rvert}+f_{\lvert\rvert}}$	$28.0^{+0.4+4.4+5.1+3.0+2.3+0.9}_{-0.6-4.5-4.0-2.7-3.1-0.8}$	$-2.3^{+0.2+0.3+0.5+0.2+0.2+0.0}_{-0.3-0.4-1.2-0.3-0.2-0.1}$
$\mathcal{A}^{\rm dir}_{CP}(\perp)(\%)$	$\frac{\bar f_\perp-f_\perp}{\bar f_\perp+f_\perp}$	$27.3^{+0.4+4.3+3.0+3.0+2.3+0.9}_{-0.6-4.6-3.3-2.7-3.2-0.8}$	$-2.5^{+0.2+0.4+0.6+0.2+0.3+0.1}_{-0.2-0.3-1.1-0.2-0.2-0.0}$

$$\mathcal{B}(B^0_d \to f_1(1285)f_1(1285)) = 6.64^{+8.70}_{-4.25} \times 10^{-7},$$
$$\mathcal{B}(B^0_s \to f_1(1285)f_1(1285)) = 3.70^{+3.49}_{-2.39} \times 10^{-6}, \quad (24)$$

$$\mathcal{B}(B^0_d \to f_1(1285)f_1(1420)) = 5.05^{+5.85}_{-3.34} \times 10^{-7},$$
$$\mathcal{B}(B^0_s \to f_1(1285)f_1(1420)) = 7.50^{+6.94}_{-4.67} \times 10^{-6}, \quad (25)$$

$$\mathcal{B}(B^0_d \to f_1(1420)f_1(1420)) = 1.00^{+1.05}_{-0.62} \times 10^{-7},$$
$$\mathcal{B}(B^0_s \to f_1(1420)f_1(1420)) = 3.37^{+3.27}_{-2.18} \times 10^{-5}, \quad (26)$$

where all the errors arising from the input parameters have been added in quadrature.

As aforementioned, the $B^0_d \to f_1 f_1$ decays have been investigated in the QCDF approach [22]. The numerical results with large errors presented in [22] can be read as follows[4]:

$$\mathcal{B}(B^0_d \to f_1(1285)f_1(1285)) = 0.2^{+0.2+2.5}_{-0.1-0.0} \times 10^{-6}, \quad (27)$$

$$\mathcal{B}(B^0_d \to f_1(1285)f_1(1420)) = 0.05^{+0.05+0.63}_{-0.00-0.00} \times 10^{-6}, \quad (28)$$

$$\mathcal{B}(B^0_d \to f_1(1420)f_1(1420)) = 0.01^{+0.01+0.06}_{-0.00-0.00} \times 10^{-6}. \quad (29)$$

The largest errors are from the parametrized hard spectator scattering and annihilation diagrams, as mentioned in [22]. Note that the parametrization of these contributions are inferred from those in the $B \to VV$ decays in the QCDF approach due to the similar behavior between the vector meson and the $^3P_1$ axial-vector one. One can see that the $B^0_d \to f_1 f_1$ decay rates predicted in the PQCD and QCDF approaches are roughly consistent with each other within large uncertainties, although, in terms of the central values, the branching ratios of the latter two modes in the QCDF approach are smaller than those in the PQCD approach with one order. It is worth pointing out that the dramatically different central values of these B^0_d decays, especially the latter two modes, by an order of magnitude in the QCDF and PQCD approaches maybe mainly resulted from the different hard scales, that is, the largest running scale $\mu = t_{\rm max}$ in the PQCD approach, while the fixed hard scale $\mu = m_b$ in the QCDF approach, and from the different treatments on the hard spectator interactions and the annihilation diagrams, that is, those contributions are quantitatively calculated in the PQCD approach, while they are roughly parametrized in the QCDF approach due to end point singularity.

According to the mixing scheme in Eq. (1) with referenced value $\phi_{f_1} = 24°$, one can easily find that the $f_1(1285)$ is predominated by the f_n component, while the $f_1(1420)$ is governed by the f_s component. Hence, for the $B^0_d \to f_1 f_1$ decays, it could be naïvely anticipated that the $B^0_d \to f_1(1285)f_1(1285)$ $[B^0_d \to f_1(1420)f_1(1420)]$ mode is tree- (penguin-)diagram dominant, but with only a few percent of penguin (tree) contaminations. For the $B^0_d \to f_1(1285)f_1(1420)$ channel, both of the tree diagrams and the penguin ones contribute evidently to the decay rate simultaneously. The decay amplitudes induced by the tree diagrams and the penguin diagrams for the $B^0_d \to f_1 f_1$ decays have been collected and can be seen clearly in the Table IV. To clarify the above expectations, we present the CP-averaged branching ratios in the PQCD approach without considering the tree contributions for the considered $B^0_d \to f_1 f_1$ decays, namely, $\mathcal{B}(B^0_d \to f_1(1285)f_1(1285)) = 1.63 \times 10^{-7}$, $\mathcal{B}(B^0_d \to f_1(1285)f_1(1420)) = 3.29 \times 10^{-7}$,

[4]As discussed in [10], the predictions in the QCDF approach for the $B \to f_1 M$ decays [6,22] with M being the pseudoscalar, vector, and axial-vector mesons provided in the second entry could be quoted to make effective comparisons to those given in the quark-flavor basis, i.e., Eq. (1), with a positive angle in the PQCD approach.

TABLE IV. Decay amplitudes(in units of 10^{-3} GeV^3) of the $B^0_d \to f_1 f_1$ modes with three polarizations in the PQCD approach, where only the central values are quoted for clarification. Note that the numerical results in the parentheses are the corresponding amplitudes without annihilation contributions.

Decay modes	$B^0_d \to f_1(1285)f_1(1285)$		$B^0_d \to f_1(1285)f_1(1420)$		$B^0_d \to f_1(1420)f_1(1420)$	
Contributions	Tree diagrams	Penguin diagrams	Tree diagrams	Penguin diagrams	Tree diagrams	Penguin diagrams
A_L	$0.463-i0.005$ $(0.299-i0.133)$	$0.253-i0.306$ $(0.219-i0.056)$	$0.292-i0.003$ $(0.189-i0.084)$	$-0.285+i0.102$ $(-0.198+i0.124)$	$0.092-i0.001$ $(0.059-i0.026)$	$-0.024-i0.132$ $(-0.168+i0.089)$
A_N	$-0.109-i0.441$ $(-0.116-i0.447)$	$-0.047+i0.203$ $(-0.024+i0.050)$	$-0.069-i0.278$ $(-0.073-i0.281)$	$-0.278+i0.282$ $(-0.262+i0.184)$	$-0.022-i0.087$ $(-0.023-i0.089)$	$-0.162+i0.134$ $(-0.160+i0.106)$
A_T	$-0.236-i0.964$ $(-0.228-i0.964)$	$-0.114+i0.413$ $(-0.065+i0.102)$	$-0.149-i0.607$ $(-0.143-i0.607)$	$-0.581+i0.565$ $(-0.549+i0.366)$	$-0.047-i0.191$ $(-0.045-i0.191)$	$-0.341+i0.267$ $(-0.333+i0.210)$

and $\mathcal{B}(B^0_d \to f_1(1420)f_1(1420)) = 0.86 \times 10^{-7}$ with about 75%, 35%, and 15% reduction, respectively. Here, only the central values are quoted for clarifications.

In principle, the $B^0_d \to f_1 f_1$ decay rates could be accessible at the LHCb and/or Belle-II experiments with accumulating a large number of $B^0_d \bar{B}^0_d$ events in the near future, after all, the $B^0_d \to K^+K^-$ with decay rate $1.3 \pm 0.5 \times 10^{-7}$ and $B^0_s \to \pi^+\pi^-$ with branching ratio $7.6 \pm 1.9 \times 10^{-7}$ [1,40,53] have been measured at LHCb. But, by considering the secondary decay process of $f_1(1285)$, namely, $\mathcal{B}(f_1(1285) \to \eta\pi^+\pi^-) \sim 35\%$ [1] or $\mathcal{B}(f_1(1285) \to 2\pi^0\pi^+\pi^-) \sim 22.3\%$ [1], then the $B^0_d \to f_1(1285)f_1(1285)$ channel have to be detected through the processes $B^0_d \to f_1(1285)(\to\eta\pi^+\pi^-)f_1(1285)(\to\eta\pi^+\pi^-)$ or $B^0_d \to f_1(1285)(\to 2\pi^0\pi^+\pi^-)f_1(1285)(\to 2\pi^0\pi^+\pi^-)$ with the branching ratios under the narrow width approximation,

$$\begin{aligned}&\mathcal{B}(B^0_d \to (\eta\pi^+\pi^-)_{f_1(1285)}(\eta\pi^+\pi^-)_{f_1(1285)})\\&\equiv \mathcal{B}(B^0_d \to f_1(1285)f_1(1285)) \cdot \mathcal{B}^2(f_1(1285) \to \eta\pi^+\pi^+),\\&\approx 0.81^{+1.07}_{-0.52} \times 10^{-7},\end{aligned} \tag{30}$$

$$\begin{aligned}&\mathcal{B}(B^0_d \to (2\pi^0\pi^+\pi^-)_{f_1(1285)}(2\pi^0\pi^+\pi^-)_{f_1(1285)})\\&\equiv \mathcal{B}(B^0_d \to f_1(1285)f_1(1285)) \cdot \mathcal{B}^2(f_1(1285) \to 2\pi^0\pi^+\pi^-),\\&\approx 0.33^{+0.43}_{-0.21} \times 10^{-7}.\end{aligned} \tag{31}$$

It seems that the above two results are too small to be measured experimentally in the near future.

However, the $B^0_s \to f_1 f_1$ decays have large branching ratios in the order of $10^{-6} \sim 10^{-5}$, which are expected to be measured in the near future at LHCb and Belle-II experiments. Unlike the $B^0_d \to f_1 f_1$ decays, the $B^0_s \to f_1 f_1$ ones are almost dominated by the pure penguin contributions just with the tiny while negligible tree pollution, which can be clearly seen from the decay amplitudes presented in the Table V. Furthermore, when the contributions from tree diagrams are turned off for the $B^0_s \to f_1 f_1$ decays, the CP-averaged branching ratios, in terms of the central values, will change slightly as follows,

$$\mathcal{B}(B^0_s \to f_1(1285)f_1(1285)) = 3.78 \times 10^{-6}, \tag{32}$$

$$\mathcal{B}(B^0_s \to f_1(1285)f_1(1420)) = 7.43 \times 10^{-6}, \tag{33}$$

$$\mathcal{B}(B^0_s \to f_1(1420)f_1(1420)) = 3.40 \times 10^{-5}. \tag{34}$$

Relative to the dominant $f_1(1285) \to \eta\pi\pi$ decay, the decay rate for the dominant $f_1(1420) \to K\bar{K}\pi$ process is not yet available.[5] Therefore, it is not easy to exactly estimate the branching ratios of $B^0_s \to f_1(1285)f_1(1420)$ and $f_1(1420)f_1(1420)$ decays via the resonant channels $B^0_s \to (\eta\pi^+\pi^-)_{f_1(1285)}(K^0_S K^+\pi^-)_{f_1(1420)}$ and $B^0_s \to (K^0_S K^+\pi^-)_{f_1(1420)}(K^0_S K^+\pi^-)_{f_1(1420)}$. Fortunately, as discussed in Ref. [55], the only decay modes of the $f_1(1420)$ were assumed as $\bar{K}K^*$, $a_0(980)\pi$, and $\phi\gamma$, and the decay rate of $f_1(1420) \to K^*\bar{K}$ was given as about 96%, then the branching ratio could be naïvely assumed as $\mathcal{B}(f_1(1420) \to K^0_S K^\pm\pi^\mp) \approx 64\%$. Then, similarly, under the narrow width approximation, the $B^0_s \to f_1(1285)(\to\eta\pi^+\pi^-)f_1(1420)(\to K^0_S K^+\pi^-)$ and $B^0_s \to f_1(1420)(\to K^0_S K^+\pi^-)f_1(1420)(\to K^0_S K^+\pi^-)$ processes have the branching ratios as follows:

$$\begin{aligned}&\mathcal{B}(B^0_s \to (\eta\pi^+\pi^-)_{f_1(1285)}(K^0_S K^+\pi^-)_{f_1(1420)})\\&\equiv \mathcal{B}(B^0_s \to f_1(1420)f_1(1420)) \cdot \mathcal{B}(f_1(1285) \to \eta\pi^+\pi^-)\\&\quad \cdot \mathcal{B}(f_1(1420) \to K^0_S K^+\pi^-) \approx 1.68^{+1.56}_{-1.04} \times 10^{-6},\end{aligned} \tag{35}$$

$$\begin{aligned}&\mathcal{B}(B^0_s \to (K^0_S K^+\pi^-)_{f_1(1420)}(K^0_S K^+\pi^-)_{f_1(1420)})\\&\equiv \mathcal{B}(B^0_s \to f_1(1420)f_1(1420)) \cdot \mathcal{B}^2(f_1(1420) \to K^0_S K^+\pi^-)\\&\approx 1.38^{+1.34}_{-0.89} \times 10^{-5}.\end{aligned} \tag{36}$$

[5]Due to the currently unknown nature [1] and the different understanding [54] of the $f_1(1420)$, we just take the absolutely dominant mode, i.e., $f_1(1420) \to \bar{K}K^*$ into account. Then, by including the secondary decay chain $K^* \to K\pi$ under the narrow width approximation, the branching ratio of the strong decay $f_1(1420) \to \bar{K}K^* \to K^0_S K^\pm\pi^\mp$ could be naïvely estimated as $\mathcal{B}(f_1(1420) \to \bar{K}K^*) \cdot \mathcal{B}(K^* \to K^\pm\pi^\mp)$.

TABLE V. Same as Table IV but for the $B_s^0 \to f_1 f_1$ modes.

Decay modes	$B_s^0 \to f_1(1285)f_1(1285)$		$B_s^0 \to f_1(1285)f_1(1420)$		$B_s^0 \to f_1(1420)f_1(1420)$	
Contributions	Tree diagrams	Penguin diagrams	Tree diagrams	Penguin diagrams	Tree diagrams	Penguin diagrams
A_L	$-0.003+i0.048$ $(-0.051+i0.020)$	$-2.202+i0.976$ $(-1.530-i0.060)$	$0.096-i0.007$ $(0.065-i0.025)$	$2.784-i1.006$ $(2.679+i0.221)$	$0.061-i0.014$ $(0.051-i0.020)$	$-1.598+i2.199$ $(-0.792-i0.400)$
A_N	$0.023+i0.074$ $(0.021+i0.073)$	$-0.612-i0.279$ $(-0.891+i0.117)$	$-0.026-i0.091$ $(-0.027-i0.092)$	$-0.055+i1.318$ $(0.868+i0.043)$	$-0.021-i0.072$ $(-0.021-i0.073)$	$3.193-i2.745$ $(1.739-i0.726)$
A_T	$0.040+i0.158$ $(0.042+i0.159)$	$-1.241-i0.592$ $(-1.827+i0.209)$	$-0.055-i0.202$ $(-0.053-i0.202)$	$-0.140+i2.663$ $(1.723+i0.095)$	$-0.042-i0.159$ $(-0.042-i0.159)$	$6.695-i5.424$ $(3.732-i1.353)$

Certainly, these two large values as given in Eqs. (35) and (36) are believed to be detectable at LHCb experiments, as well as at Belle-II ones in the near future.

Different from the ideal mixing between ω and ϕ in the vector sector, both of $f_1(1285)$ and $f_1(1420)$ mesons have some admixtures of f_s and f_n correspondingly. Therefore, though the similarity of the distribution amplitudes between the f_1 states and the $\omega(\phi)$ mesons has been observed [22], relative to the $B_{d,s}^0 \to \omega(\phi)\omega(\phi)$ and $B_{d,s}^0 \to f_1\omega(\phi)$ decays, the more complicated interferences among the $B_{d,s}^0 \to f_n f_n, f_n f_s$, and $f_s f_s$ are involved in the $B_{d,s}^0 \to f_1 f_1$ decays, as presented explicitly in the Eqs. (13)–(15) and Eqs. (19)–(21). In other words, it is not easy to naïvely anticipate the constructive or destructive interferences in the $B_{d,s}^0 \to f_1 f_1$ decays just like those in the $B_{d,s}^0 \to \omega(\phi)\omega(\phi)$, and $B_{d,s}^0 \to f_1\omega(\phi)$ ones. But, as observed in the Table VI, the $B_s^0 \to f_n f_n$ channel has a small longitudinal while two tiny and negligible transverse amplitudes, which would make the interferences in the $B_s^0 \to f_1 f_1$ decays more easy to be explored. Therefore, it can still be expected that the nearly pure penguin $B_s^0 \to f_1(1420)f_1(1420)$ decay with a large branching ratio could provide useful information to constrain the $B_s^0 - \bar{B}_s^0$ mixing phase, even to find new physics signal beyond the standard model complementarily.

As clearly seen in the Tables I–III, the numerical results calculated in the PQCD approach suffer from large uncertainties induced by the less constrained distribution amplitudes of the involved hadrons. At the same time, frankly speaking, it is worthy of stressing that the large errors presented in the Tables I–III for the considered $B_{d,s}^0 \to f_1 f_1$ decays are mainly induced by the decay constants, Gegenbauer moments, even the mixing angle of the f_1 mesons. In light of these large uncertainties, we then define some interesting ratios of the branching ratios for the decay modes. As generally expected, if the modes in a ratio have similar dependence on a specific input parameter, the error induced by the uncertainty of this input parameter will be largely canceled in the ratio, even if one cannot make an explicit factorization for this parameter. Furthermore, from the experimental side, we know that the ratios of the branching ratios generally could be measured with a better accuracy than that for the individual branching ratios. The relevant ratios about the decay rates of the considered $B_{d,s}^0 \to f_1 f_1$ decays can be read as follows:

TABLE VI. Decay amplitudes(in units of 10^{-3} GeV^3) for flavor states $B_{d,s}^0 \to f_n f_n, f_n f_s$, and $f_s f_s$ of the $B_{d,s}^0 \to f_1 f_1$ modes with three polarizations in the PQCD approach, where only the central values are quoted for clarification. Note that the numerical results in the parentheses are the corresponding amplitudes of $\bar{B}_{d,s}^0 \to f_n f_n, f_n f_s$, and $f_s f_s$.

Decays	$B_d^0 \to f_1 f_1$			$B_s^0 \to f_1 f_1$		
Flavor states	$B_d^0 \to f_n f_n$	$B_d^0 \to f_n f_s$	$B_d^0 \to f_s f_s$	$B_s^0 \to f_n f_n$	$B_s^0 \to f_n f_s$	$B_s^0 \to f_s f_s$
A_L A_L	$0.433-i0.162$ $(-0.176-i0.315)$	$-0.336+i0.159$ $(-0.350-i0.125)$	$0.121-i0.151$ $(0.193-i0.021)$	$-0.411+i0.484$ $(-0.470+i0.416)$	$2.278-i0.068$ $(2.080-i0.059)$	$-2.235+i1.786$ $(-2.235+i1.786)$
A_N	$-0.242-i0.133$ $(-0.427+i0.418)$	$-0.246+i0.152$ $(-0.282-i0.067)$	$0.002-i0.002$ $(0.003+i0.000)$	$-0.006+i0.005$ $(-0.008+i0.002)$	$1.923-i0.553$ $(1.912-i0.280)$	$1.833-i2.142$ $(1.833-i2.142)$
A_T	$-0.523-i0.332$ $(-0.902+i0.887)$	$-0.509+i0.302$ $(-0.573-i0.147)$	$0.001-i0.004$ $(0.004-i0.002)$	$-0.003+i0.006$ $(0.000+i0.007)$	$3.997-i1.059$ $(3.959-i0.468)$	$3.858-i4.259$ $(3.858-i4.259)$

$$R_1^{sd}[f_1(1285)f_1(1420)] \equiv \frac{\mathcal{B}(B_s^0 \to f_1(1285)f_1(1420))_{\rm PQCD}}{\mathcal{B}(B_d^0 \to f_1(1285)f_1(1420))_{\rm PQCD}}, \approx 14.85^{+0.63}_{-0.21}(\omega_B)^{+9.96}_{-5.89}(f_M)^{+2.23}_{-4.18}(a_{f_1})^{+1.40}_{-0.65}(\phi_{f_1})^{+0.28}_{-0.52}(a_t)^{+0.26}_{-0.30}(V), \quad (37)$$

$$R_2^{sd}[f_1(1285)f_1(1285)] \equiv \frac{\mathcal{B}(B_s^0 \to f_1(1285)f_1(1285))_{\rm PQCD}}{\mathcal{B}(B_d^0 \to f_1(1285)f_1(1285))_{\rm PQCD}}, \approx 5.57^{+0.80}_{-0.64}(\omega_B)^{+2.80}_{-1.61}(f_M)^{+0.66}_{-1.47}(a_{f_1})^{+0.58}_{-0.34}(\phi_{f_1})^{+0.68}_{-0.71}(a_t)^{+0.26}_{-0.25}(V), \quad (38)$$

$$R_3^{sd}[f_1(1420)f_1(1420)] \equiv \frac{\mathcal{B}(B_s^0 \to f_1(1420)f_1(1420))_{\rm PQCD}}{\mathcal{B}(B_d^0 \to f_1(1420)f_1(1420))_{\rm PQCD}}, \approx 3.37^{+0.27}_{-0.32}(\omega_B)^{+1.58}_{-1.11}(f_M)^{+0.66}_{-1.33}(a_{f_1})^{+0.79}_{-0.75}(\phi_{f_1})^{+0.19}_{-0.17}(a_t)^{+0.01}_{-0.00}(V) \times 10^2, \quad (39)$$

$$R_4^{dd}[f_1(1285)/f_1(1420)] \equiv \frac{\mathcal{B}(B_d^0 \to f_1(1285)f_1(1285))_{\rm PQCD}}{\mathcal{B}(B_d^0 \to f_1(1285)f_1(1420))_{\rm PQCD}}, \approx 1.31^{+0.05}_{-0.04}(\omega_B)^{+0.20}_{-0.22}(f_M)^{+0.36}_{-0.15}(a_{f_1})^{+0.04}_{-0.05}(\phi_{f_1})^{+0.14}_{-0.12}(a_t)^{+0.04}_{-0.05}(V), \quad (40)$$

$$R_5^{ss}[f_1(1420)/f_1(1285)] \equiv \frac{\mathcal{B}(B_s^0 \to f_1(1285)f_1(1420))_{\rm PQCD}}{\mathcal{B}(B_s^0 \to f_1(1285)f_1(1285))_{\rm PQCD}}, \approx 2.03^{+0.28}_{-0.22}(\omega_B)^{+0.68}_{-0.53}(f_M)^{+0.34}_{-0.48}(a_{f_1})^{+0.12}_{-0.08}(\phi_{f_1})^{+0.01}_{-0.00}(a_t)^{+0.00}_{-0.01}(V), \quad (41)$$

$$R_6^{dd}[f_1(1285)/f_1(1420)] \equiv \frac{\mathcal{B}(B_d^0 \to f_1(1285)f_1(1420))_{\rm PQCD}}{\mathcal{B}(B_d^0 \to f_1(1420)f_1(1420))_{\rm PQCD}}, \approx 5.05^{+0.11}_{-0.19}(\omega_B)^{+0.54}_{-0.60}(f_M)^{+0.01}_{-0.38}(a_{f_1})^{+1.17}_{-1.08}(\phi_{f_1})^{+0.04}_{-0.00}(a_t)^{+0.11}_{-0.09}(V), \quad (42)$$

$$R_7^{ss}[f_1(1420)/f_1(1285)] \equiv \frac{\mathcal{B}(B_s^0 \to f_1(1420)f_1(1420))_{\rm PQCD}}{\mathcal{B}(B_s^0 \to f_1(1285)f_1(1420))_{\rm PQCD}}, \approx 4.49^{+0.35}_{-0.45}(\omega_B)^{+0.02}_{-0.01}(f_M)^{+0.17}_{-0.39}(a_{f_1})^{+0.68}_{-0.42}(\phi_{f_1})^{+0.14}_{-0.10}(a_t)^{+0.01}_{-0.00}(V), \quad (43)$$

$$R_8^{dd}[f_1(1285)/f_1(1420)] \equiv \frac{\mathcal{B}(B_d^0 \to f_1(1285)f_1(1285))_{\rm PQCD}}{\mathcal{B}(B_d^0 \to f_1(1420)f_1(1420))_{\rm PQCD}}, \approx 6.64^{+0.00}_{-0.10}(\omega_B)^{+1.79}_{-1.78}(f_M)^{+1.18}_{-0.78}(a_{f_1})^{+1.20}_{-1.26}(\phi_{f_1})^{+0.72}_{-0.59}(a_t)^{+0.35}_{-0.31}(V), \quad (44)$$

$$R_9^{ss}[f_1(1420)/f_1(1285)] \equiv \frac{\mathcal{B}(B_s^0 \to f_1(1420)f_1(1420))_{\rm PQCD}}{\mathcal{B}(B_s^0 \to f_1(1285)f_1(1285))_{\rm PQCD}}, \approx 9.11^{+2.07}_{-1.79}(\omega_B)^{+3.05}_{-2.36}(f_M)^{+1.92}_{-2.74}(a_{f_1})^{+1.02}_{-1.18}(\phi_{f_1})^{+0.31}_{-0.16}(a_t)^{+0.02}_{-0.02}(V). \quad (45)$$

Generally speaking, it should be noted that the errors arising from the parameters, in particular f_{f_n} and f_{f_s} and $a_2^{\parallel}$ and $a_1^{\perp}$, cannot be reduced effectively in the ratios because of the significant interferences among the decay amplitudes of $B^0_{d,s} \to f_n f_n, f_n f_s$, and $f_s f_s$. Nevertheless, we still expect that the LHCb and/or Belle-II experiments could perform the measurements with enough precision on these ratios in the future, in order to give some essential constraints on the input parameters or the mixing angle ϕ_{f_1}.

From the numerical results for the decay amplitudes of the $B^0_{d,s} \to f_1 f_1$ decays and the $B^0_{d,s} \to f_n f_n, f_n f_s$, and $f_s f_s$ flavor states collected in the Tables IV–VI, one can find that the constructive or destructive interferences with different extents in the considered decays could vary with

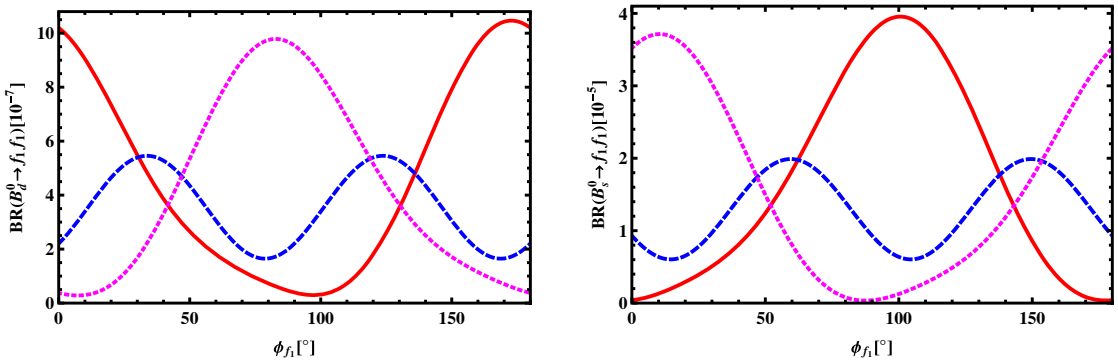

FIG. 2. Dependence of the CP-averaged $B^0_{d,s} \to f_1 f_1$ branching ratios on ϕ_{f_1} in the PQCD approach, in which the red, solid line, the blue, dashed line, and the magenta, dotted line correspond to the $B^0_{d,s}$ decays with final states $f_1(1285)f_1(1285)$, $f_1(1285)f_1(1420)$, and $f_1(1420)f_1(1420)$, respectively.

the mixing angle ϕ_{f_1} between f_n and f_s in the quark-flavor basis. To see the variation clearly with the mixing angle, we show the CP-averaged branching ratios $\mathcal{B}(B^0_{d,s} \to f_1 f_1)$ varying with $\phi_{f_1} \in [0, \pi]$ in Fig. 2. It is of great interest to find that the line-shapes of $\mathcal{B}(B^0_d \to f_1(1285)f_1(1285))$ and $\mathcal{B}(B^0_s \to f_1(1420)f_1(1420))$ in the PQCD approach vary with ϕ_{f_1} similar to each other, but with a quasi mirror symmetry, i.e., the red, solid line on the l.h.s. and the magenta, dotted line on the r.h.s., as shown in Fig. 2. The differences between these two lines are indeed induced by the dramatic interferences arising from the contributions from $B^0_d \to f_n f_s$ to the former while that from $B^0_s \to f_n f_s$ to the latter. And similar phenomena also appear in the line shapes of $\mathcal{B}(B^0_d \to f_1(1285)f_1(1420))$ and $\mathcal{B}(B^0_s \to f_1(1285)f_1(1420))$, as well as of $\mathcal{B}(B^0_d \to f_1(1420)f_1(1420))$ and $\mathcal{B}(B^0_s \to f_1(1285)f_1(1285))$. This picture really displays the different interferences mainly from $B^0_d \to f_n f_n$ and $B^0_d \to f_n f_s$ to the $B^0_d \to f_1 f_1$ decays while from $B^0_s \to f_s f_s$ and $B^0_s \to f_n f_s$ to the $B^0_s \to f_1 f_1$ decays. Of course, as given in the Table VI, the decay amplitudes from $B^0_d \to f_s f_s$ and $B^0_s \to f_n f_n$ in the longitudinal polarization also contribute to the $B^0_{d,s} \to f_1 f_1$ decays. Therefore, it is expected that, if the precise f_n and f_s distribution amplitudes are available, then the mixing angle ϕ_{f_1} could be constrained by the near future measurements on the large $B^0_s \to f_1 f_1$ decay rates associated with the interferences as exhibited in Fig. 2, and vice versa.

B. CP-averaged polarization fractions

Now, we turn to the calculations for the polarization fractions of the $B^0_{d,s} \to f_1 f_1$ decays. Based on the helicity amplitudes $A_i (i = L, N, T)$, we can equivalently define the amplitudes in the transversity basis as follows:

$$\mathcal{A}_L = \xi m^2_{B^0_{d,s}} A_L, \qquad \mathcal{A}_\parallel = \xi\sqrt{2} m^2_{B^0_{d,s}} A_N,$$
$$\mathcal{A}_\perp = \xi m^2_{B^0_{d,s}} r^2_{f_1} \sqrt{2(r^2-1)} A_T, \tag{46}$$

for the longitudinal, parallel, and perpendicular polarizations, respectively, with the normalization factor $\xi = \sqrt{G_F^2 P_c/(16\pi m_B^2 \Gamma)}$ and the ratio $r = P_2 \cdot P_3/(m_{f_1} \cdot m_{f_1})$. These amplitudes satisfy the relation,

$$|\mathcal{A}_L|^2 + |\mathcal{A}_\parallel|^2 + |\mathcal{A}_\perp|^2 = 1, \tag{47}$$

following the summation in Eq. (23). Since the transverse-helicity contributions can manifest themselves through polarization observables, we therefore define CP-averaged fractions in three polarizations f_L, $f_\parallel$, and $f_\perp$ as the following,

$$f_{L,\parallel,\perp} \equiv \frac{|\mathcal{A}_{L,\parallel,\perp}|^2}{|\mathcal{A}_L|^2 + |\mathcal{A}_\parallel|^2 + |\mathcal{A}_\perp|^2} = |\mathcal{A}_{L,\parallel,\perp}|^2. \tag{48}$$

With the above transversity amplitudes shown in Eq. (46), the relative phases $\phi_\parallel$ and $\phi_\perp$ can be defined as

$$\phi_\parallel = \arg\frac{\mathcal{A}_\parallel}{\mathcal{A}_L}, \qquad \phi_\perp = \arg\frac{\mathcal{A}_\perp}{\mathcal{A}_L}. \tag{49}$$

From the Tables I–III, one can clearly find that four of the considered $B^0_{d,s} \to f_1 f_1$ decays are dominated by the transverse contributions, while the other two are governed by the longitudinal ones, whose values for the polarization fractions f_L and $f_T (= 1 - f_L)$ can be explicitly read as follows,

$$f_L(B^0_d \to f_1(1285)f_1(1285)) = 27.7^{+19.7}_{-11.4}\%,$$
$$f_T(B^0_d \to f_1(1285)f_1(1285)) = 72.3^{+8.4}_{-14.1}\%, \tag{50}$$

$$f_L(B^0_d \to f_1(1285) f_1(1420)) = 18.0^{+14.1}_{-6.0}\%,$$
$$f_T(B^0_d \to f_1(1285) f_1(1420)) = 81.9^{+4.6}_{-10.0}\%, \quad (51)$$

$$f_L(B^0_d \to f_1(1420) f_1(1420)) = 12.4^{+21.3}_{-8.1}\%,$$
$$f_T(B^0_d \to f_1(1420) f_1(1420)) = 87.6^{+6.0}_{-15.3}\%, \quad (52)$$

$$f_L(B^0_s \to f_1(1420) f_1(1420)) = 10.6^{+10.3}_{-4.5}\%,$$
$$f_T(B^0_s \to f_1(1420) f_1(1420)) = 89.4^{+3.3}_{-7.6}\%, \quad (53)$$

and

$$f_L(B^0_s \to f_1(1285) f_1(1285)) = 78.9^{+5.2}_{-7.5}\%,$$
$$f_T(B^0_s \to f_1(1285) f_1(1285)) = 21.1^{+5.4}_{-3.8}\%, \quad (54)$$

$$f_L(B^0_s \to f_1(1285) f_1(1420)) = 59.0^{+10.0}_{-13.3}\%,$$
$$f_T(B^0_s \to f_1(1285) f_1(1420)) = 40.9^{+9.6}_{-7.0}\%, \quad (55)$$

in which all the errors from various parameters have been added in quadrature. These predicted CP-averaged polarization fractions will be tested at LHCb and/or Belle-II to further explore the decay mechanism with helicities associated with experimental confirmations on the decay rates.

In Ref. [22], the longitudinal polarization fractions of the $B^0_d \to f_1 f_1$ decays have been calculated in the QCDF approach,

$$f_L(B^0_d \to f_1(1285) f_1(1285))_{\rm QCDF} = 0.66^{+0.07}_{-0.84}, \quad (56)$$

$$f_L(B^0_d \to f_1(1285) f_1(1420))_{\rm QCDF} = 0.57^{+0.10}_{-0.66}, \quad (57)$$

$$f_L(B^0_d \to f_1(1420) f_1(1420))_{\rm QCDF} = 0.68^{+0.23}_{-0.58}. \quad (58)$$

As far as the central values are considered, the results in the QCDF approach exhibit the dominance of the longitudinal decay amplitudes, which are very contrary to those in the PQCD approach at leading order. However, when the large uncertainties are taken into account, then one can find that the transverse contributions can also govern these $B^0_d \to f_1 f_1$ decays possibly.

In order to show explicitly the interferences among different flavor states contributing to the $B^0_{d,s} \to f_1 f_1$ decays in three polarizations, we collect their corresponding decay amplitudes, namely, $A_L(B^0_{d,s} \to f_n f_n)$, $A_N(B^0_{d,s} \to f_n f_s)$, and $A_T(B^0_{d,s} \to f_s f_s)$ in the Table VI, and the resultant amplitudes for the physical states, i.e., $A_L(B^0_{d,s} \to f_1 f_1)$, $A_N(B^0_{d,s} \to f_1 f_1)$, and $A_T(B^0_{d,s} \to f_1 f_1)$, with differentiating them from tree diagrams and from penguin diagrams in the Tables IV and V. From these results quoted with only central values, one can easily observe that, generally speaking, the significantly constructive [destructive] interferences govern the $B^0_d \to f_1 f_1$ and $B^0_s \to f_1(1420) f_1(1420)$ $[B^0_s \to f_1(1285) f_1(1285)]$ decays transversely [longitudinally]. While for the $B^0_s \to f_1(1285) f_1(1420)$ mode, the interferences are slightly moderate within errors on both longitudinal and transverse polarizations.

Unfortunately, no data or theoretical predictions for the considered $B^0_s \to f_1 f_1$ decays are available nowadays. It is therefore expected that our predictions in the PQCD approach would be confronted with future LHCb and/or Belle-II experiments, as well as the theoretical comparisons within the framework of QCDF, soft-collinear effective theory [56], and so forth.

Although, as aforementioned, the global agreement with data for $B \to VV$ decays has been greatly improved in the PQCD approach theoretically [48] by picking up higher power r_i^2 terms that were previously neglected, it seems that the predictions about the polarization fractions for the $B^0_{d,s} \to f_1 f_1$ decays cannot be understood similarly as the $B^0_{d,s} \to \omega\omega, \phi\phi$ decays [48] due to the constructive and/or destructive interferences with different extents.

Let us take the $B^0_{d,s} \to f_1(1285) f_1(1285)$ and $B^0_{d,s} \to f_1(1420) f_1(1420)$ decays as examples to clarify the differences from the vector decays of $B^0_{d,s} \to \omega\omega$ and $B^0_{d,s} \to \phi\phi$ with ideal mixing in the PQCD approach at leading order [48]. As we know, with the referenced value $\phi_{f_1} = 24°$, the physical states $f_1(1285)$ and $f_1(1420)$ are predominated by the component of f_n and f_s with a factor about $\cos\phi_{f_1} = 0.914$. Thus, due to the similar behavior of the vector and $^3P_1$-axial-vector mesons, the $B^0_{d,s} \to f_1(1285) f_1(1285)$ and $B^0_{d,s} \to f_1(1420) f_1(1420)$ decays, in principle, could provide similar phenomena when the interferences from the f_s and f_n component are turned off correspondingly. Numerically, the $B^0_{d,s} \to f_1(1285) f_1(1285)$ and $B^0_{d,s} \to f_1(1420) f_1(1420)$ decay rates and the longitudinal polarization fractions without the relevant interferences mentioned above could be read as

(i) Without the interferences from the f_s component,

$$\mathcal{B}(B^0_d \to f_1(1285) f_1(1285)) = 1.03 \times 10^{-6} \cdot \cos^2\phi_{f_1},$$
$$f_L(B^0_d \to f_1(1285) f_1(1285)) = 17.5\%, \quad (59)$$

$$\mathcal{B}(B^0_s \to f_1(1285) f_1(1285)) = 4.04 \times 10^{-7} \cdot \cos^2\phi_{f_1},$$
$$f_L(B^0_s \to f_1(1285) f_1(1285)) = 100\%. \quad (60)$$

(ii) Without the interferences from the f_n component,

$$\mathcal{B}(B^0_d \to f_1(1420) f_1(1420)) = 0.37 \times 10^{-7} \cdot \cos^2\phi_{f_1},$$
$$f_L(B^0_d \to f_1(1420) f_1(1420)) = 99.9\%, \quad (61)$$

$$\mathcal{B}(B^0_s \to f_1(1420) f_1(1420)) = 3.52 \times 10^{-5} \cdot \cos^2\phi_{f_1},$$
$$f_L(B^0_s \to f_1(1420) f_1(1420)) = 22.8\%. \quad (62)$$

The ideal mixing, i.e., $\phi_{f_1} = 0°$, in the above equations would give the cases like $B^0_{d,s} \to \omega\omega$ and $B^0_{d,s} \to \phi\phi$ decays, because the $B^0_{d,s} \to f_1(1285)f_1(1285)$ decays just receive the contributions from the flavor amplitude $B^0_{d,s} \to f_n f_n$ while the $B^0_{d,s} \to f_1(1420)f_1(1420)$ ones just from the $B^0_{d,s} \to f_s f_s$ correspondingly. Here, it is noted that, in comparison to the decay constants $f_\omega = 0.187$ GeV, $f^T_\omega = 0.151$ GeV and $f_\phi = 0.215$ GeV, $f^T_\phi = 0.186$ GeV for the vector ω and ϕ [57], the decay constants $f_{f_n} = 0.193$ GeV and $f_{f_s} = 0.230$ GeV [50] can remarkably enhance the contributions on the transverse polarization in the $B^0_d \to f_n f_n$ and $B^0_s \to f_s f_s$ decays, respectively, which finally result in the small longitudinal polarization fractions already presented in the above equations. Meanwhile, one can easily observe that the interferences from the $B^0_d \to f_n f_s$ and $B^0_d \to f_s f_s$ amplitudes contribute destructively to the $B^0_d \to f_1(1285)f_1(1285)$ decay rate with 23%, while those from the $B^0_s \to f_n f_s$ and $B^0_s \to f_n f_n$ amplitudes contribute constructively to the $B^0_s \to f_1(1420)f_1(1420)$ branching ratio with 15%. For the pure annihilation decays $B^0_d \to f_s f_s$ and $B^0_s \to f_n f_n$, as shown in the Table VI, both of them are absolutely governed by the longitudinal contributions and the polarization fractions are about 100%, which are almost the same as those in the $B^0_d \to \phi\phi$ and $B^0_s \to \omega\omega$ decays correspondingly.

As presented in the Eqs. (8)–(21) and in the Tables IV–VI, one can find that, except for the other four penguin-dominated modes, the $B^0_d \to f_1(1285)f_1(1285)$ and $B^0_d \to f_1(1285)f_1(1420)$ decays received the contributions arising from the color-suppressed tree amplitudes with different extents. To our knowledge, the $B^0_d \to \rho^0\rho^0$ decay dominated by the color-suppressed tree amplitude has a small decay rate and a similarly small longitudinal polarization fraction in the PQCD approach at leading order that cannot be comparable to the measurements. Nevertheless, the partial next-to-leading order contributions from vertex corrections, quark loop, and chromomagnetic penguin diagrams [58], and the evolution from the Glauber-gluon associated with the transverse-momentum-dependent wave functions [28] could remarkably enhance the branching ratio and the longitudinal polarization fractions simultaneously. Then the theoretical predictions could be consistent well with the measurements given by *BABAR* [59] and LHCb [60] experiments within errors.[6] Therefore, the future examinations at LHCb and/or Belle-II experiments on these two mentioned channels sensitive to the above-mentioned color-suppressed tree amplitudes could help to identify the needs of the possible next-to-leading order corrections. Of course, this issue has to be left for future study elsewhere.

In addition, we present the relative phases (in units of rad) $\phi_\parallel$ and $\phi_\perp$ of the $B^0_{d,s} \to f_1 f_1$ decays for the first time. The numerical results can be seen explicitly in the Tables I–III. Of course, these predictions have to await for the future tests because no measurements have been available until now.

C. Direct *CP*-violating asymmetries

Now we come to the evaluations of direct *CP*-violating asymmetries of the $B^0_{d,s} \to f_1 f_1$ decays in the PQCD approach. As for the direct *CP* violation $\mathcal{A}^{\rm dir}_{CP}$, it is defined as

$$\mathcal{A}^{\rm dir}_{CP} \equiv \frac{\bar{\Gamma} - \Gamma}{\bar{\Gamma} + \Gamma} = \frac{|\bar{A}_{\rm final}|^2 - |A_{\rm final}|^2}{|\bar{A}_{\rm final}|^2 + |A_{\rm final}|^2}, \tag{63}$$

where Γ and $A_{\rm final}$ stand for the decay rate and the decay amplitude of $B^0_{d,s} \to f_1 f_1$, while $\bar{\Gamma}$ and $\bar{A}_{\rm final}$ denote the charge conjugation ones, correspondingly. Meanwhile, according to Ref. [62], the direct-induced *CP* asymmetries can also be studied with the help of helicity amplitudes. Usually, we need to combine three polarization fractions, as shown in Eq. (48), with those corresponding conjugation ones of *B* decays and then to quote the resultant six observables to define direct *CP* violations of $B^0_{d,s} \to f_1 f_1$ decays in the transversity basis as follows:

$$\mathcal{A}^{{\rm dir},\ell}_{CP} = \frac{\bar{f}_\ell - f_\ell}{\bar{f}_\ell + f_\ell}, \tag{64}$$

where $\ell = L, \parallel, \perp$ and the definition of $\bar{f}$ is the same as that in Eq. (48) but for the corresponding $\bar{B}^0_{d,s}$ decays.

Using Eq. (63), we calculate the direct *CP*-violating asymmetries in the $B^0_{d,s} \to f_1 f_1$ decays and present the results as shown in Tables I–III. Based on these numerical values, some comments are in order:

(1) The direct *CP*-violating asymmetries within still large theoretical errors for the $B^0_{d,s} \to f_1 f_1$ decays could be read straightforwardly from the Tables I–III as follows,

$$\begin{aligned} \mathcal{A}^{\rm dir}_{CP}(B^0_d \to f_1(1285)f_1(1285)) &= 26.5^{+14.0}_{-19.9}\%, \\ \mathcal{A}^{\rm dir}_{CP}(B^0_s \to f_1(1285)f_1(1285)) &= -0.3^{+1.3}_{-1.3}\%, \end{aligned} \tag{65}$$

$$\begin{aligned} \mathcal{A}^{\rm dir}_{CP}(B^0_d \to f_1(1285)f_1(1420)) &= 54.7^{+4.4}_{-10.1}\%, \\ \mathcal{A}^{\rm dir}_{CP}(B^0_s \to f_1(1285)f_1(1420)) &= 2.8^{+0.8}_{-0.9}\%, \end{aligned} \tag{66}$$

$$\begin{aligned} \mathcal{A}^{\rm dir}_{CP}(B^0_d \to f_1(1420)f_1(1420)) &= 25.4^{+10.6}_{-15.8}\%, \\ \mathcal{A}^{\rm dir}_{CP}(B^0_s \to f_1(1420)f_1(1420)) &= -1.9^{+0.6}_{-0.8}\%, \end{aligned} \tag{67}$$

[6] It should be mentioned that previously the Belle collaboration reported a small longitudinal polarization fraction of the $B^0_d \to \rho^0\rho^0$ decay [61], which is in good agreement with the values in the PQCD approach at leading order [48], but is different dramatically to that in the QCDF approach [22,62,63] and the soft-collinear effective theory [64]. It means that a refined measurement on this small longitudinal polarization fraction is very important at the Belle-II experiment.

where all the errors from various parameters as specified previously have been added in quadrature. For the former decays with $\Delta S = 0$, as exhibited in the Table IV, the considerable tree or penguin contaminations lead to the large direct CP asymmetries. While for the latter decays with $\Delta S = 1$, as displayed in the Table V, the negligible tree pollution result in the very small direct CP violations. Currently, all these direct CP violations seem hard to be detected in the near future experimentally due to the small decay rates for the former decays and due to the tiny CP asymmetries for the latter ones.

(ii) For the $B^0_s \to f_1(1285)f_1(1285)$ and $B^0_s \to f_1(1285)f_1(1420)$ decays, there exist the large direct CP-violating asymmetries in both transverse polarizations, namely, parallel and perpendicular, with still large theoretical errors as follows:

$$\mathcal{A}_{CP}^{\mathrm{dir},\parallel}(B^0_s \to f_1(1285)f_1(1285)) = 9.1^{+7.5}_{-6.6}\%,$$
$$\mathcal{A}_{CP}^{\mathrm{dir},\perp}(B^0_s \to f_1(1285)f_1(1285)) = 8.6^{+7.9}_{-6.7}\%, \quad (68)$$

and

$$\mathcal{A}_{CP}^{\mathrm{dir},\parallel}(B^0_s \to f_1(1285)f_1(1420)) = 13.6^{+5.0}_{-5.8}\%,$$
$$\mathcal{A}_{CP}^{\mathrm{dir},\perp}(B^0_s \to f_1(1285)f_1(1420)) = 14.8^{+5.5}_{-6.4}\%, \quad (69)$$

which may be easily accessible associated with the large decay rates in the order of $10^{-6} \sim 10^{-5}$ within theoretical errors. Other predictions about the direct CP violations in every polarization for the considered $B^0_{d,s} \to f_1 f_1$ decays could be found out in the Tables I–III explicitly, we here will not list them individually. These results could be tested in the (near) future at LHCb, Belle-II, and other facilities such as the Circular Electron-Positron Collider.

At last, we shall give some remarks on the important annihilation contributions.[7] In particular, the penguin annihilation contributions was proposed to explain the polarization anomaly in the $B \to \phi K^*$ decays in standard model [65]. Subsequently, more studies about the $B \to VV$ decays based on the rich data were made in a systematic manner, and the penguin-dominated channels were further found to need the annihilation contributions to a great extent [22,48,62–64,66]. It is worth pointing out that, because of similar behavior between the vector and the $^3P_1$-axial-vector mesons, the authors proposed the similar annihilation contributions, as in the $B \to VV$ decays, to estimate the $B \to A(^3P_1)V$ and $A(^3P_1)A(^3P_1)$ decay rates and polarization fractions [22].

Therefore, we shall explore the important contributions from weak annihilation diagrams to the $B^0_{d,s} \to f_1 f_1$ decays considered in this work. In order to clearly examine the important annihilation contributions, we present the explicit decay amplitudes in Tables IV and V decomposed as tree diagrams and penguin diagrams with and without annihilation contributions in three polarizations. To show the variations of the considered $B^0_{d,s} \to f_1 f_1$ decays with no inclusion of the contributions from annihilation diagrams, we shall list the observables numerically such as the CP-averaged branching ratios, the polarization fractions, and the direct CP-violating asymmetries by taking only the factorizable emission plus the nonfactorizable emission decay amplitudes into account in the PQCD approach.

(1) Branching ratios

Without the contributions from annihilation diagrams, then the branching ratios will turn out to be

$$\mathcal{B}(B^0_d \to f_1(1285)f_1(1285)) = 5.00^{+6.72}_{-3.38} \times 10^{-7},$$
$$\mathcal{B}(B^0_s \to f_1(1285)f_1(1285)) = 2.60^{+2.63}_{-1.85} \times 10^{-6}, \quad (70)$$

$$\mathcal{B}(B^0_d \to f_1(1285)f_1(1420)) = 3.72^{+4.55}_{-2.61} \times 10^{-7},$$
$$\mathcal{B}(B^0_s \to f_1(1285)f_1(1420)) = 4.83^{+4.09}_{-3.05} \times 10^{-6}, \quad (71)$$

$$\mathcal{B}(B^0_d \to f_1(1420)f_1(1420)) = 0.95^{+1.07}_{-0.70} \times 10^{-7},$$
$$\mathcal{B}(B^0_s \to f_1(1420)f_1(1420)) = 0.65^{+0.71}_{-0.43} \times 10^{-5}. \quad (72)$$

(2) Longitudinal polarization fractions

By neglecting the weak annihilation contributions, the CP-averaged longitudinal polarization fractions of the $B^0_{d,s} \to f_1 f_1$ decays are written as

$$f_L(B^0_d \to f_1(1285)f_1(1285)) = 16.7^{+11.6}_{-4.3}\%,$$
$$f_L(B^0_s \to f_1(1285)f_1(1285)) = 45.8^{+8.1}_{-11.3}\%, \quad (73)$$

$$f_L(B^0_d \to f_1(1285)f_1(1420)) = 13.3^{+7.3}_{-2.2}\%,$$
$$f_L(B^0_s \to f_1(1285)f_1(1420)) = 74.6^{+12.8}_{-13.9}\%, \quad (74)$$

[7] In principle, as part of the power corrections, the nonfactorizable emission diagrams could also contribute to the observables. However, associated with the symmetric behavior from the leading-twist distribution amplitudes of the f_n and f_s states, the mentioned contributions are much smaller than those from the annihilation diagrams due to the cancelation between the two nonfactorizable emission diagrams, e.g., see Fig. 1(c) with hard gluon from valence antiquark and 1(d) with hard gluon from valence quark, respectively. Numerically, by taking the $B^0_s \to f_1(1420)f_1(1420)$ decay rate $\mathcal{B}(B^0_s \to f_1(1420)f_1(1420)) \approx 3.37^{+3.27}_{-2.18} \times 10^{-5}$ as an example, it is found that $\mathcal{B}(B^0_s \to f_1(1420)f_1(1420)) \approx 0.65^{+0.71}_{-0.43} \times 10^{-5}$ without the contributions arising from the annihilation diagrams and $\mathcal{B}(B^0_s \to f_1(1420)f_1(1420)) \approx 0.01^{+0.04}_{-0.01} \times 10^{-5}$ without the nonfactorizable emission and annihilation contributions. Therefore, we here emphasize the more important power corrections, i.e., annihilation contributions, in this paper.

$$f_L(B_d^0 \to f_1(1420)f_1(1420)) = 21.0^{+4.9}_{-4.8}\%,$$
$$f_L(B_s^0 \to f_1(1420)f_1(1420)) = 6.0^{+16.8}_{-6.3}\%. \quad (75)$$

(3) Direct CP-violating asymmetries

Without the contributions arising from annihilation type diagrams, the direct CP-violating asymmetries are then given as

$$\mathcal{A}_{CP}^{\rm dir}(B_d^0 \to f_1(1285)f_1(1285)) = -1.2^{+12.3}_{-18.4}\%,$$
$$\mathcal{A}_{CP}^{\rm dir}(B_s^0 \to f_1(1285)f_1(1285)) = -4.7^{+0.5}_{-1.6}\%, \quad (76)$$

$$\mathcal{A}_{CP}^{\rm dir}(B_d^0 \to f_1(1285)f_1(1420)) = 39.1^{+1.9}_{-5.3}\%,$$
$$\mathcal{A}_{CP}^{\rm dir}(B_s^0 \to f_1(1285)f_1(1420)) = -3.7^{+2.0}_{-3.2}\%, \quad (77)$$

$$\mathcal{A}_{CP}^{\rm dir}(B_d^0 \to f_1(1420)f_1(1420)) = 29.8^{+6.7}_{-8.1}\%,$$
$$\mathcal{A}_{CP}^{\rm dir}(B_s^0 \to f_1(1420)f_1(1420)) = -2.4^{+0.5}_{-1.6}\%. \quad (78)$$

In the above equations, all the errors from various parameters have been added in quadrature. Generally speaking, within the still large theoretical errors, for the branching ratios for example, by combining the results as presented in the Eqs. (24)–(26), it seems that the numerical results with and without the important annihilation contributions could be consistent with each other in a 2σ standard deviation. However, in light of the central values about the observables for the $B_{d,s}^0 \to f_1 f_1$ decays, the results collected in the Eqs. (24)–(26), (50)–(55), (65)–(67), and (70)–(78) clearly show that

(i) the annihilation diagrams can contribute to the $B_{d,s}^0 \to f_1 f_1$ decay rates with different ratios from the least 5% to the largest 80%. Specifically, once the annihilation contributions are turned off, then the CP-averaged branching ratios of the $B_{d,s}^0 \to f_1 f_1$ decays will decrease about 25% for the $B_d^0 \to f_1(1285)f_1(1285)$ and $B_d^0 \to f_1(1285)f_1(1420)$ modes; and reduce around 30% and 35% for the $B_s^0 \to f_1(1285)f_1(1285)$ and $B_s^0 \to f_1(1285)f_1(1420)$ ones, respectively. The annihilation diagrams can enhance $\mathcal{B}(B_s^0 \to f_1(1420)f_1(1420))$ from 0.65×10^{-5} to 3.37×10^{-5}.

(ii) Indeed, the annihilation diagrams can modify the polarization fractions of the $B_{d,s}^0 \to f_1 f_1$ decays with different extents. Without the contributions from the annihilation diagrams, it is found that the $B_s^0 \to f_1(1285)f_1(1420)$ channel remains longitudinal polarization dominated but with a 26% enhancement, the $B_d^0 \to f_1(1285)f_1(1285)$, $B_d^0 \to f_1(1285)f_1(1420)$, $B_s^0 \to f_1(1420)f_1(1420)$, and $B_d^0 \to f_1(1420)f_1(1420)$ decays remains transverse polarization dominated but with a 40%, 26%, 42% reduction of f_L, and a near 70% enhancement of f_L, respectively, and the $B_s^0 \to f_1(1285)f_1(1285)$ mode goes from a large longitudinal polarization fraction to a slightly larger transverse one than one half.

(iii) As claimed in [67], the annihilation diagrams in the heavy B meson decays could contribute a large imaginary part, as shown in the Tables IV and V, and act as the main source of large strong phase in the PQCD approach. Therefore, the absence of the contributions from annihilation diagrams change the interferences highly between the weak and strong phases in the $B_{d,s}^0 \to f_1 f_1$ decays and finally results in the significant variations of the direct CP-violating asymmetries, even the positive or negative signs.

IV. CONCLUSIONS AND SUMMARY

In short, we have analyzed the $B_s^0 \to f_1 f_1$ decays for the first time in the quark-flavor basis with the PQCD approach. We obtained the small decay rates that are hard to be measured in the CKM suppressed $B_d^0 \to f_1 f_1$ decays while the large branching ratios that are easy to be accessible in the CKM favored $B_s^0 \to f_1 f_1$ ones due to the interferences with different extents among the flavor decay amplitudes $B_{d,s}^0 \to f_n f_n$, $f_n f_s$, and $f_s f_s$. Particularly, the $B_s^0 \to f_1(1420)f_1(1420)$ decay with a large branching ratio in the order of 10^{-5} is expected to be measured through the $B_s^0 \to (K_S^0 K^{\pm}\pi^{\mp})_{f_1(1420)}(K_S^0 K^{\pm}\pi^{\mp})_{f_1(1420)}$ channel. Our numerical results of the observables such as the CP-averaged branching ratios, the polarization fractions, and the direct CP-violating asymmetries indicate that the weak annihilation diagrams play important roles in understanding the dynamics in these $B_{d,s}^0 \to f_1 f_1$ decays in the PQCD approach. Of course, these predictions in the PQCD approach await for the confirmations from the future examinations, which could help us to understand the annihilation decay mechanism in vector-vector and vector-axial-vector B decays in depth. We explored the dependence of $\mathcal{B}(B_{d,s}^0 \to f_1 f_1)$ on the mixing angle ϕ_{f_1} in the quark-flavor basis and found the interesting line shapes to hint useful information. In light of the large theoretical errors induced by the unconstrained inputs, we also defined nine ratios of the $B_{d,s}^0 \to f_1 f_1$ decay rates to await for the (near) future measurements at LHCb and/or Belle-II, even other facilities, e.g., Circular Electron-Positron Collider. Note that the large uncertainties of the predicted branching ratios are canceled to a large extent in several ratios. Then the mixing angle ϕ_{f_1} between the flavor states f_n and f_s could be further constrained, which would finally help pin down the θ_{K_1} angle to understand the properties of the light axial-vector mesons more precisely.

ACKNOWLEDGMENTS

The authors thank Hai-Yang Cheng and Ju-Jun Xie for helpful discussions. This work is supported in part by the National Natural Science Foundation of China under

Grants No. 11765012, No. 11775117, No. 11705159, and No. 11975195, by the Qing Lan Project of Jiangsu Province under Grant No. 9212218405, by the Natural Science Foundation of Shandong province under the Grants No. ZR2018JL001 and No. ZR2019JQ04, by the Project of Shandong Province Higher Educational Science and Technology Program under Grant No. 2019KJJ007, and by the Research Fund of Jiangsu Normal University under Grant No. HB2016004. Z. J. is supported by Postgraduate Research & Practice Innovation Program of Jiangsu Province (Grant No. KYCX20_2225).

APPENDIX: WAVE FUNCTIONS AND DISTRIBUTION AMPLITUDES

The heavy B meson is usually treated as a heavy-light system and its light-cone wave function can generally be defined as [26,68]

$$\Phi_B = \frac{i}{\sqrt{2N_c}}\{(\not{P} + m_B)\gamma_5 \phi_B(x, k_T)\}_{\alpha\beta}, \tag{A1}$$

where α, β are the color indices; P is the momentum of B meson; N_c is the color factor; and k_T is the intrinsic transverse momentum of the light quark in B meson. Recent developments on the B meson wave function and its distribution amplitude can refer to, e.g., the Refs. [69].

The B meson distribution amplitude in the impact b (not to be confused with the heavy quark b. Here, b is the conjugate space coordinate of transverse momentum k_T) space has been proposed as [26]

$$\phi_B(x,b) = N_B x^2(1-x)^2 \exp\left[-\frac{1}{2}\left(\frac{x m_B}{\omega_B}\right)^2 - \frac{\omega_B^2 b^2}{2}\right], \tag{A2}$$

and widely adopted, for example, in [8–10,26,28,31,33,48]. This B meson distribution amplitude obeys the following normalization condition,

$$\int_0^1 dx \phi_B(x, b=0) = \frac{f_B}{2\sqrt{2N_c}}, \tag{A3}$$

where f_B is the decay constant of the B meson related to the normalization factor N_B. For the B^0_d meson, the shape parameter ω_B was fixed at 0.40 GeV with $f_B = 0.19$ GeV and $N_B = 91.745$ by combining the rich data and plenties of PQCD calculations on the observables of B^+ and B^0_d mesons' decays [26,68]. Here, the assumption of isospin symmetry has been made. For the B^0_s meson, a somewhat larger momentum fraction is adopted due to the heavier s quark, relative to the lightest u or d quark in the B^+ or B^0_d mesons. Therefore, by considering a small SU(3) symmetry-breaking effect, we adopt the shape parameter $\omega_B = 0.50$ GeV with $f_B = 0.23$ GeV for the B^0_s meson [33], and the corresponding normalization constant is $N_B = 63.67$. In order to estimate the theoretical uncertainties induced by the shape parameters, we also consider varying the shape parameter ω_B by 10%, that is, $\omega_B = 0.40 \pm 0.04$ GeV for B^0_d meson and $\omega_B = 0.50 \pm 0.05$ GeV for the B^0_s meson, respectively.

The wave functions for the light flavor $f_{n(s)}$ state of the axial-vector f_1 mesons can be written as [23,49],

$$\Phi^L_{f_{n(s)}} = \frac{1}{\sqrt{2N_c}}\gamma_5\{m_{f_{n(s)}} \epsilon\!\!/_L \phi_{f_{n(s)}}(x) + \epsilon\!\!/_L P\!\!/ \phi^t_{f_{n(s)}}(x) + m_{f_{n(s)}} \phi^s_{f_{n(s)}}(x)\}_{\alpha\beta}, \tag{A4}$$

$$\Phi^T_{f_{n(s)}} = \frac{1}{\sqrt{2N_c}}\gamma_5\{m_{f_{n(s)}} \epsilon\!\!/_T \phi^v_{f_{n(s)}}(x) + \epsilon\!\!/_T P\!\!/ \phi^T_{f_{n(s)}}(x) + m_{f_{n(s)}} i\epsilon_{\mu\nu\rho\sigma}\gamma_5\gamma^\mu \epsilon\!\!/^\nu_T n^\rho v^\sigma \phi^a_{f_{n(s)}}(x)\}_{\alpha\beta}, \tag{A5}$$

for longitudinal and transverse polarizations, respectively, with the polarization vectors ϵ_L and ϵ_T of $f_{n(s)}$, satisfying $P \cdot \epsilon = 0$. x denotes the momentum fraction carried by quarks in $f_{n(s)}$, $n = (1, 0, \mathbf{0}_T)$ and $v = (0, 1, \mathbf{0}_T)$ are dimensionless lightlike unit vectors, and $m_{f_{n(s)}}$ stands for the mass of light axial-vector flavor state $f_{n(s)}$. In addition, we adopt the convention $\epsilon^{0123} = 1$ for the Levi-Civita tensor $\epsilon^{\mu\nu\alpha\beta}$.

The twist-2 light cone distribution amplitudes can generally be expanded as the Gegenbauer polynomials [23]:

$$\phi_{f_{n(s)}}(x) = \frac{f_{f_{n(s)}}}{2\sqrt{2N_c}} 6x(1-x)\left[1 + a_2^{\parallel}\frac{3}{2}(5(2x-1)^2 - 1)\right], \tag{A6}$$

$$\phi^T_{f_{n(s)}}(x) = \frac{f_{f_{n(s)}}}{2\sqrt{2N_c}} 6x(1-x)[3a_1^{\perp}(2x-1)]. \tag{A7}$$

For the twist-3 ones, we use the following form as in Ref. [49]:

$$\phi^s_{f_{n(s)}}(x) = \frac{f_{f_{n(s)}}}{4\sqrt{2N_c}}\frac{d}{dx}[6x(1-x)(a_1^{\perp}(2x-1))], \tag{A8}$$

$$\phi^t_{f_{n(s)}}(x) = \frac{f_{f_{n(s)}}}{2\sqrt{2N_c}}\left[\frac{3}{2}a_1^{\perp}(2x-1)(3(2x-1)^2 - 1)\right], \tag{A9}$$

$$\phi^v_{f_{n(s)}}(x) = \frac{f_{f_{n(s)}}}{2\sqrt{2N_c}}\left[\frac{3}{4}(1 + (2x-1)^2)\right], \tag{A10}$$

$$\phi^a_{f_{n(s)}}(x) = \frac{f_{f_{n(s)}}}{8\sqrt{2N_c}}\frac{d}{dx}[6x(1-x)], \tag{A11}$$

where $f_{f_{n(s)}}$ is the "normalization" constant for the flavor state $f_{n(s)}$ on both longitudinal and transverse polarizations, and the Gegenbauer moments $a_2^{\parallel}$ and $a_1^{\perp}$ are as follows:

$$a_2^{\parallel} = \begin{cases} -0.05^{+0.03}_{-0.03} & (\text{for } f_n), \\ 0.10^{+0.15}_{-0.19} & (\text{for } f_s), \end{cases} \qquad a_1^{\perp} = \begin{cases} -1.08^{+0.48}_{-0.48} & (\text{for } f_n), \\ 0.30^{+0.00}_{-0.33} & (\text{for } f_s). \end{cases} \tag{A12}$$

[1] P. A. Zyla *et al.* (Particle Data Group), Prog. Theor. Exp. Phys. **2020**, 083C01 (2020); 63. Pseudoscalar and pseudovector meson in the 1400 MeV region, mini-review by C. Amsler and A. Masoni in the Reviews of Particle Physics.
[2] K. Chen, C. Q. Pang, X. Liu, and T. Matsuki, Phys. Rev. D **91**, 074025 (2015).
[3] C. Amsler and N. A. Tornqvist, Phys. Rep. **389**, 61 (2004).
[4] R. Aaij *et al.* (LHCb Collaboration), Phys. Rev. Lett. **112**, 091802 (2014).
[5] H. Y. Cheng, Phys. Lett. B **707**, 116 (2012).
[6] H. Y. Cheng and K. C. Yang, Phys. Rev. D **76**, 114020 (2007).
[7] T. Feldmann, arXiv:1408.0300; W. Wang, R. H. Li, and C. D. Lü, Phys. Rev. D **78**, 074009 (2008).
[8] X. Liu, Z. T. Zou, and Z. J. Xiao, Phys. Rev. D **90**, 094019 (2014).
[9] X. Liu and Z. J. Xiao, Phys. Rev. D **89**, 097503 (2014).
[10] X. Liu, Z. J. Xiao, J. W. Li, and Z. T. Zou, Phys. Rev. D **91**, 014008 (2015).
[11] F. E. Close and A. Kirk, Phys. Rev. D **91**, 114015 (2015).
[12] F. E. Close and A. Kirk, Z. Phys. C **76**, 469 (1997).
[13] D. M. Li, H. Yu, and Q. X. Shen, Chin. Phys. Lett. **17**, 558 (2000).
[14] G. Gidal, J. Boyer, F. Butler, D. Cords, G. S. Abrams, D. Amidei, A. R. Baden, T. Barklow *et al.*, Phys. Rev. Lett. **59**, 2012 (1987).
[15] W. S. Carvalho, A. S. de Castro, and A. C. B. Antunes, J. Phys. A **35**, 7585 (2002).
[16] D. M. Li, B. Ma, and H. Yu, Eur. Phys. J. A **26**, 141 (2005).
[17] K. C. Yang, Phys. Rev. D **78**, 034018 (2008).
[18] K. C. Yang, Phys. Rev. D **84**, 034035 (2011).
[19] J. J. Dudek, R. G. Edwards, B. Joo, M. J. Peardon, D. G. Richards, and C. E. Thomas, Phys. Rev. D **83**, 111502 (2011).
[20] S. Stone and L. Zhang, Phys. Rev. Lett. **111**, 062001 (2013).
[21] H. Y. Cheng, *Proc. Sci.*, Hadron2013 (2013) 090 [arXiv:1311.2370].
[22] H. Y. Cheng and K. C. Yang, Phys. Rev. D **78**, 094001 (2008); **79**, 039903(E) (2009).
[23] K. C. Yang, Nucl. Phys. **B776**, 187 (2007).
[24] J. J. Dudek, R. G. Edwards, P. Guo, and C. E. Thomas, Phys. Rev. D **88**, 094505 (2013).
[25] X. Liu, Z. J. Xiao, and Z. T. Zou, Phys. Rev. D **94**, 113005 (2016).
[26] Y. Y. Keum, H.-n. Li, and A. I. Sanda, Phys. Lett. B **504**, 6 (2001); Phys. Rev. D **63**, 054008 (2001); C. D. Lü, K. Ukai, and M. Z. Yang, Phys. Rev. D **63**, 074009 (2001); H.-n. Li, Prog. Part. Nucl. Phys. **51**, 85 (2003).
[27] Q. Chang, J. Sun, Y. Yang, and X. Li, Phys. Rev. D **90**, 054019 (2014); L. Hofer and L. Vernazza, arXiv:1212.4785; H. J. Lipkin, arXiv:1107.1888; arXiv:1105.3443; S. Chang, C. S. Kim, and J. Song, Phys. Lett. B **696**, 367 (2011); T. N. Pham, arXiv:0910.2561; S. Khalil, A. Masiero, and H. Murayama, Phys. Lett. B **682**, 74 (2009); D. Chang, C. S. Chen, H. Hatanaka, S. M. Kim, and W. Namgung, J. Korean Phys. Soc. **54**, 1457 (2009); S. Baek, C. W. Chiang, and D. London, Phys. Lett. B **675**, 59 (2009); G. Bhattacharyya, K. B. Chatterjee, and S. Nandi, Phys. Rev. D **78**, 095005 (2008); M. Imbeault, S. Baek, and D. London, Phys. Lett. B **663**, 410 (2008); C. S. Kim, S. Oh, and Y. W. Yoon, Int. J. Mod. Phys. A **23**, 3296 (2008); Phys. Lett. B **665**, 231 (2008); S. Baek, Phys. Lett. B **659**, 265 (2008); C. S. Kim, S. Oh, C. Sharma, R. Sinha, and Y. W. Yoon, Phys. Rev. D **76**, 074019 (2007); R. Fleischer, S. Recksiegel, and F. Schwab, Eur. Phys. J. C **51**, 55 (2007); R. Fleischer, arXiv:0701217; S. Baek and D. London, Phys. Lett. B **653**, 249 (2007); S. Baek, A. Datta, P. Hamel, D. London, and D. A. Suprun, AIP Conf. Proc. **805**, 318 (2006); D. Chang, C. S. Chen, H. Hatanaka, and C. S. Kim, arXiv:0510328; Y. D. Yang, R. Wang, and G. R. Lu, Phys. Rev. D **73**, 015003 (2006); R. L. Arnowitt, B. Dutta, B. Hu, and S. Oh, Phys. Lett. B **633**, 748 (2006); R. Fleischer, Int. J. Mod. Phys. A **21**, 664 (2006); C. S. Kim, S. Oh, and C. Yu, Phys. Rev. D **72**, 074005 (2005); S. Baek, P. Hamel, D. London, A. Datta, and D. A. Suprun, Phys. Rev. D **71**, 057502 (2005); A. J. Buras, R. Fleischer, S. Recksiegel, and F. Schwab, Acta Phys. Pol. B **36**, 2015 (2005); Phys. Rev. Lett. **92**, 101804 (2004); Eur. Phys. J. C **32**, 45 (2003); V. Barger, C. W. Chiang, P. Langacker, and H. S. Lee, Phys. Lett. B **598**, 218 (2004).
[28] X. Liu, H.-n. Li, and Z. J. Xiao, Phys. Rev. D **91**, 114019 (2015); **93**, 014024 (2016).
[29] G. Bell, M. Beneke, T. Huber, and X. Q. Li, J. High Energy Phys. 04 (2020) 055; *Proc. Sci.*, RADCOR2019 (2019) 032; T. Huber, S. Krankl, and X. Q. Li, J. High Energy Phys. 09 (2016) 112; G. Bell, M. Beneke, T. Huber, and X. Q. Li, Phys. Lett. B **750**, 348 (2015); G. Bell and T. Huber, J. High Energy Phys. 12 (2014) 129; M. Beneke, T. Huber, and X. Q. Li, Nucl. Phys. **B832**, 109 (2010); G. Bell, Nucl. Phys. **B795**, 1 (2008); G. Bell, Nucl. Phys. **B822**, 172 (2009); G. Bell and V. Pilipp, Phys. Rev. D **80**, 054024 (2009); G. Bell, arXiv:0705.3133.
[30] M. Beneke, G. Buchalla, M. Neubert, and C. T. Sachrajda, Phys. Rev. Lett. **83**, 1914 (1999); Nucl. Phys. **B591**, 313 (2000).
[31] H.-n. Li, Y. L. Shen, Y. M. Wang, and H. Zou, Phys. Rev. D **83**, 054029 (2011); H.-n. Li, Y. L. Shen, and Y. M. Wang, Phys. Rev. D **85**, 074004 (2012); J. High Energy Phys. 02 (2013) 008; H. C. Hu and H.-n. Li, Phys. Lett. B **718**, 1351 (2013); Z. Rui, G. Xiangdong, and C. D. Lü, Eur. Phys. J. C

72, 1923 (2012); S. Cheng, Y. Y. Fan, X. Yu, C. D. Lü, and Z. J. Xiao, Phys. Rev. D **89**, 094004 (2014); Y. L. Zhang, X. Y. Liu, Y. Y. Fan, S. Cheng, and Z. J. Xiao, Phys. Rev. D **90**, 014029 (2014); S. Cheng, Z. J. Xiao, and Y. L. Zhang, Nucl. Phys. **B896**, 255 (2015); H.-n. Li and S. Mishima, Phys. Rev. D **83**, 034023 (2011); **90**, 074018 (2014).
[32] Z. J. Xiao, D. Q. Guo, and X. F. Chen, Phys. Rev. D **75**, 014018 (2007).
[33] A. Ali, G. Kramer, Y. Li, C. D. Lü, Y. L. Shen, W. Wang, and Y. M. Wang, Phys. Rev. D **76**, 074018 (2007).
[34] M. Beneke, G. Buchalla, M. Neubert, and C. T. Sachrajda, Nucl. Phys. **B606**, 245 (2001); M. Beneke and M. Neubert, Nucl. Phys. **B675**, 333 (2003).
[35] B. H. Hong and C. D. Lü, Sci. Chin. G **49**, 357 (2006).
[36] A. V. Gritsan (*BABAR* Collaboration), eConf C **070512**, 001 (2007).
[37] H.-n. Li, Phys. Lett. B **622**, 63 (2005).
[38] H.-n. Li and S. Mishima, Phys. Rev. D **71**, 054025 (2005).
[39] H.-n. Li, C. D. Lü, and F. S. Yu, Phys. Rev. D **86**, 036012 (2012).
[40] T. Aaltonen *et al.* (CDF Collaboration), Phys. Rev. Lett. **108**, 211803 (2012); F. Ruffini, FERMILAB-THESIS-2013-02; R. Aaij *et al.* (LHCb Collaboration), J. High Energy Phys. 10 (2012) 037.
[41] Z. J. Xiao, W. F. Wang, and Y. Y. Fan, Phys. Rev. D **85**, 094003 (2012).
[42] H.-n. Li, Phys. Rev. D **66**, 094010 (2002).
[43] H.-n. Li and K. Ukai, Phys. Lett. B **555**, 197 (2003).
[44] J. Botts and G. F. Sterman, Nucl. Phys. **B325**, 62 (1989).
[45] H.-n. Li and G. F. Sterman, Nucl. Phys. **B381**, 129 (1992).
[46] G. Buchalla, A. J. Buras, and M. E. Lautenbacher, Rev. Mod. Phys. **68**, 1125 (1996).
[47] X. Liu and Z. J. Xiao, Phys. Rev. D **86**, 074016 (2012).
[48] Z. T. Zou, A. Ali, C. D. Lü, X. Liu, and Y. Li, Phys. Rev. D **91**, 054033 (2015).
[49] R. H. Li, C. D. Lü, and W. Wang, Phys. Rev. D **79**, 034014 (2009).
[50] R. C. Verma, J. Phys. G **39**, 025005 (2012).
[51] L. Wolfenstein, Phys. Rev. Lett. **51**, 1945 (1983).
[52] M. Tanabashi *et al.* (Particle Data Group), Phys. Rev. D **98**, 030001 (2018).
[53] Y. S. Amhis *et al.* (HFLAV Collaboration), arXiv:1909.12524; updated in https://hflav.web.cern.ch/.
[54] J. J. Xie (private communications).
[55] D. Barberis *et al.* (WA102 Collaboration), Phys. Lett. B **413**, 225 (1997); **440**, 225 (1998).
[56] C. W. Bauer, S. Fleming, D. Pirjol, and I. W. Stewart, Phys. Rev. D **63**, 114020 (2001); C. W. Bauer, D. Pirjol, and I. W. Stewart, Phys. Rev. D **65**, 054022 (2002).
[57] P. Ball and R. Zwicky, Phys. Rev. D **71**, 014029 (2005).
[58] H.-n. Li and S. Mishima, Phys. Rev. D **73**, 114014 (2006).
[59] B. Aubert *et al.* (*BABAR* Collaboration), Phys. Rev. D **78**, 071104 (2008).
[60] R. Aaij *et al.* (LHCb Collaboration), Phys. Lett. B **747**, 468 (2015).
[61] I. Adachi *et al.* (Belle Collaboration), Phys. Rev. D **89**, 072008 (2014); **89**, 119903(A) (2014).
[62] M. Beneke, J. Rohrer, and D. Yang, Nucl. Phys. **B774**, 64 (2007).
[63] H. Y. Cheng and C. K. Chua, Phys. Rev. D **80**, 114008 (2009).
[64] C. Wang, S. H. Zhou, Y. Li, and C. D. Lü, Phys. Rev. D **96**, 073004 (2017).
[65] A. L. Kagan, Phys. Lett. B **601**, 151 (2004).
[66] H. Y. Cheng and J. G. Smith, Annu. Rev. Nucl. Part. Sci. **59**, 215 (2009).
[67] J. Chay, H.-n. Li, and S. Mishima, Phys. Rev. D **78**, 034037 (2008).
[68] C. D. Lü and M. Z. Yang, Eur. Phys. J. C **28**, 515 (2003).
[69] W. Wang, Y. M. Wang, J. Xu, and S. Zhao, Phys. Rev. D **102**, 011502 (2020); H.-n. Li and Y. M. Wang, J. High Energy Phys. 06 (2015) 013; T. Feldmann, B. O. Lange, and Y. M. Wang, Phys. Rev. D **89**, 114001 (2014); G. Bell, T. Feldmann, Y. M. Wang, and M. W. Y. Yip, J. High Energy Phys. 11 (2013) 191.